J Neurophysiol 103: 2417–2432, 2010.
First published February 24, 2010; doi:10.1152/jn.01143.2009.

Cholinergic Modulation of Fast Inhibitory and Excitatory Transmission to Pedunculopontine Thalamic Projecting Neurons

Meijun Ye, Abdallah Hayar, Beau Strotman, and Edgar Garcia-Rill
Center for Translational Neuroscience, Department of Neurobiology and Developmental Sciences, University of Arkansas for Medical Sciences, Little Rock, Arkansas

Submitted 28 December 2009; accepted in final form 21 February 2010

Ye M, Hayar A, Strotman B, Garcia-Rill E. Cholinergic modulation of fast inhibitory and excitatory transmission to pedunculopontine thalamic projecting neurons. *J Neurophysiol* 103: 2417–2432, 2010. First published February 24, 2010; doi:10.1152/jn.01143.2009. The pedunculopontine nucleus (PPN) is part of the cholinergic arm of the reticular activating system, which is mostly active during waking and rapid-eye movement sleep. The PPN projects to the thalamus and receives cholinergic inputs from the laterodorsal tegmental nucleus and contralateral PPN. We employed retrograde labeling and whole cell recordings to determine the modulation of GABAergic, glycinergic, and glutamatergic transmission to PPN thalamic projecting neurons, and their postsynaptic responses to the nonspecific cholinergic agonist carbachol. M2 and M4 muscarinic receptor-modulated inhibitory postsynaptic responses were observed in 73% of PPN output neurons; in 12.9%, M1 and nicotinic receptor-mediated excitation was detected; and muscarinic and nicotinic-modulated fast inhibitory followed by slow excitatory biphasic responses were evident in 6.7% of cells. A significant increase in the frequency of spontaneous excitatory postsynaptic currents (EPSCs) and inhibitory postsynaptic currents during carbachol application was observed in 66.2% and 65.2% of efferent neurons, respectively. This effect was blocked by a M1 antagonist or nonselective muscarinic blocker, indicating that glutamatergic, GABAergic, and/or glycinergic neurons projecting to PPN output neurons are excited through muscarinic receptors. Decreases in the frequency of miniature EPSCs, and amplitude of electrical stimulation-evoked EPSCs, were blocked by a M2 antagonist, suggesting the presence of M2Rs at terminals of presynaptic glutamatergic neurons. Carbachol-induced multiple types of postsynaptic responses, enhancing both inhibitory and excitatory fast transmission to PPN thalamic projecting neurons through muscarinic receptors. These results provide possible implications for the generation of different frequency oscillations in PPN thalamic projecting neurons during distinct sleep-wake states.

INTRODUCTION

The pedunculopontine nucleus (PPN) is part of the cholinergic arm of the reticular activating system (RAS) and is thought to be critical for switching cortical arousal states from nonrapid eye movement (NREM) sleep to wakefulness or REM sleep (Hobson and Pace-Schott 2002). During waking and REM sleep, PPN neurons show increased firing rates (Datta and Siwek 2002), whereas decreased rates of firing are present during slow wave sleep (SWS). Early studies established that electrical or chemical stimulation of the midbrain reticular formation in the region of the PPN and its ascending projections induced "desynchronization" of the cortex (Moruzzi and Magoun 1949), which is similar to that observed during waking and REM sleep. Lesions in the region of the PPN reduced or eliminated REM sleep (Deurveilher and Hennevin 2001). In addition, systemic and intracerebral injections of cholinergic agonists were found to generate ponto-geniculo-occipital (PGO) waves prior to the onset of, and throughout, REM sleep (Datta et al. 1998; Sakai et al. 1990; Steriade et al. 1990).

The induction of cortical manifestations of waking or REM sleep by PPN stimulation are mainly mediated through its ascending projections to the thalamus, which may represent the machinery for the generation of oscillations during distinct sleep-wake states. The increase in acetylcholine concentration in "specific" thalamic nuclei following PPN stimulation appears to excite thalamocortical relay neurons and inhibit reticular thalamic neurons, which in turn, blocks spindle oscillations and delta waves appearing during NREM sleep (McCormick 1992). However, the "nonspecific" thalamocortical neurons, including centrolateral (CL) and parafascicular (Pf) cells, are the main target of PPN thalamic projections (Kobayashi and Nakamura 2003; Parent and Descarries 2008). Both "specific" and "nonspecific" thalamic nuclei are involved in sensory processing and presumably the modulation of conscious experience through the thalamocortical 40 Hz rhythm (Llinas and Ribary 2001).

In addition to medium and large cholinergic neurons, the PPN contains glutamatergic and GABAergic neurons (Clements and Grant 1990; Ford et al. 1995; Wang and Morales 2009). PPN neurons receive cholinergic input from the laterodorsal tegmental (LDT) and contralateral PPN (Semba and Fibiger 1992), GABAergic innervation from local interneurons and the substantia nigra (Saitoh et al. 2003), and glutamatergic excitation from nuclei in the mesopontine area and thalamus (Steininger et al. 1992; Stevens et al. 1992) and probably local glutamatergic neurons as well. In terms of electrophysiological properties, three types of PPN neurons have been identified, type I cells are known to have only low threshold calcium spike (LTS) channels, type II have only hyperpolarization activated transient potassium outward currents (Ia), while type III have both Ia and LTS (Kang and Kitai 1990; Leonard and Llinas 1990). Seventy-three percent of type II and 36% of type III neurons were found to be cholinergic, whereas, all type I cells were noncholinergic (Takakusaki et al. 1996, 1997). Other than these three types, a fourth group of PPN neuron has been reported that show neither A nor LTS currents (Kang and Kitai 1990; Kim et al. 2009). Our previous sharp intracellular recordings from 12 to 21 day PPN neurons showed a decrease in the proportion of type III neurons with development, apparently differentiating into type I neurons (Kobayashi et al. 2003). The membrane properties and synaptic input of PPN

Address for reprint requests and other correspondence: E. Garcia-Rill, Center for Translational Neuroscience, Dept. of Neurobiology and Developmental Sciences, University of Arkansas for Medical Sciences, Slot 847, 4301 W. Markham St., Little Rock, AR 72205 (E-mail: GarciaRillEdgar@uams.edu).

 0022-3077/10 Copyright © 2010 The American Physiological Society

Downloaded from jn.physiology.org on August 15, 2010

neurons appear to be essential for determining their firing patterns that may be modulated by cholinergic input during different cortical arousal states.

Although the importance of PPN neurons in the modulation of sleep-wake cycles has been established, the exact mechanisms underlying these functions remain a mystery. Understanding the synaptic interactions within the PPN, and also between the PPN and other nuclei, is an essential step for unveiling this mystery. In this study, we employed retrograde labeling, whole cell patch clamp recording, and immunohistochemical techniques to investigate how cholinergic input modulates GABAergic and glutamatergic synaptic transmission, and probably glycinergic as well, to PPN thalamic projecting neurons, with additional consideration of their electrophysiological and neurotransmitter phenotypes.

METHODS

Retrograde labeling of PPN thalamic projecting neurons

Pups aged 9–14 days from adult timed-pregnant Sprague-Dawley rats (280–350 g) were anesthetized with 65 mg/kg ip ketamine until tail pinch reflexes were absent. Retrograde labeling of PPN neurons was performed using a picospritzer (Parker Hannifin) for pressure injection of ~4 μl of green fluorescent latex microsphere retrobeads (Lumafluor, Durham, NC) into the thalamus, using a glass pipette with ~60–70 μm tip diameter. The green microspheres showed little diffusion and produced well-defined injection sites. The stereotaxic coordinates of the injection sites were (mm, relative to Bregma): AP −2 to −3, L +0.5 to +0.8, DV −5.5 to −6.5. The same animals were used to prepare brain slices for patch-clamp recordings 24–72 h after injection. Injection sites for each experiment were confirmed by visualization using a Nikon AZ-100 microscope (Nikon Instruments, Melville, NY) and NIS Elements AR imaging and analysis software. Only neurons from animals with injection sites within thalamocortical nuclei were included in the statistical analysis. All animal use procedures were approved by the University of Arkansas for Medical Sciences Institutional Animal Care and Use Committee and comply with the ethical standards described in the National Institutes of Health guide.

Slice preparation

Pups aged 10–15 days were anesthetized with ketamine (70 mg/kg im) until tail pinch and corneal reflexes were absent. They were decapitated and the brain rapidly removed and blocked in cooled, oxygenated (95% O_2-5% CO_2) sucrose artificial cerebrospinal fluid (sucrose-ACSF). The block of tissue was glued onto a stage, and 400 μm parasagittal slices of the thalamus and brain stem were cut with a Vibratome 1000 plus with a 900R refrigeration system (Vibratome Instruments, St. Louis, MO) in cooled oxygenated sucrose-ACSF. Slices were allowed to equilibrate at room temperature in oxygenated ACSF for ≥1 h before recording. The ACSF consisted of (in mM) 117 NaCl, 4.7 KCl, 1.2 $MgCl_2$, 2.5 $CaCl_2$, 24.9 $NaHCO_3$, and 11.5 glucose. The sucrose-ACSF was composed of (in mM) 233.7 sucrose, 26 $NaHCO_3$, 8 $MgCl_2$, 0.5 $CaCl_2$, 20 glucose, and 0.4 ascorbic acid.

Whole cell patch clamp recordings

Whole cell patch clamp recordings were acquired using borosilicate glass pipettes (with filament) with resistance of 8–12 MΩ that were pulled on a Sutter P-87 puller (Sutter Instrument, Novato, CA) and filled with normal pipette solution containing (in mM) 124 K-gluconate, 10 phosphocreatine di tris salt, 10 HEPES, 0.2 EGTA, 4 MgATP, 0.3 Na_2GTP, and 0.5% neurobiotin for the direct postsynaptic effect, and excitatory postsynaptic currents (EPSCs), studies. K-gluconate was substituted with equimolar concentration of KCl for recording inhibitory PSCs (IPSCs). The osmolarity of the pipette solution was adjusted to ~270–290 mosM and pH to 7.4. Slices were recorded at 30°C while superfused (~1.5 ml/min) with oxygenated ACSF. No series resistance compensation was performed in this study. The pipette series resistance may increase during an experiment due to an increase in pipette clogging or a slight drift of the cell surface away from the pipette. However, neurons with access resistance exceeding 20 MΩ were excluded from the analysis. Neurons were visualized using an upright microscope (Nikon FN1 with ×40 water immersion lens, ×1–2 magnifying turret, and Gibraltar platform, Nikon Instruments, Melville, NY) equipped for epifluorescence and near-infrared differential interference contrast optics. The location of recorded cells was confirmed using a ×4 objective lens before and after recording. Retrogradely labeled PPN output neurons were identified as containing fluorescent beads under fluorescence illumination. All recorded analog signals were low-pass filtered at 2 kHz using a Multiclamp 700B amplifier and digitized at 5 kHz using a Digidata-1440A and pClamp 10 software (Molecular Devices, Union City, CA). Bath-applied drugs were administered to the slice via a peristaltic pump (Cole-Parmer, Vernon Hills, IL) and a three-way valve system. To determine the intrinsic membrane properties of cells, a series of depolarizing and hyperpolarizing steps were applied at −60 mV holding potential (HP) in both current-clamp mode (−100-60 pA, 20 pA steps, 500 ms in duration) and voltage-clamp mode (−110-10 mV, 15 mV steps, 500 ms in duration). The presence of a potassium A current (Ia) was determined by testing whether a significant transient outward current is produced in response to a depolarizing voltage step to −60 or −45 mV which was preceded by a 500 ms negative voltage step to −110 mV. To test the effects of neuroactive agents, every 20 s, the membrane potential was held at a hyperpolarized level (HP = −100 mV) for 500 ms to determine changes in input resistance (R_{in}), then a 1,000 ms voltage ramp from −100 to −30 mV was applied to test the current-voltage relationship of the activated currents. For the identification of electrical stimulation-evoked EPSCs and IPSCs, the membrane potential was held at −70 mV to prevent the generation of action potentials, and every 10 s, a hyperpolarizing step from −70 to −110 mV was applied to determine changes in R_{in}.

Electrical stimulation

To evoke EPSCs and IPSCs, electrical stimulation was applied using a bipolar tungsten microelectrode driven by a Grass S88 stimulator (Grass Instruments) connected to a SIU5 stimulus isolation unit (Grass Instruments, West Warwick, RI). The stimulating electrode (200 kΩ resistance, 50 μm intertip distance) was placed in the PPN, 50–200 μm away from recorded neurons. The membrane potential of recorded neurons was held at −70 mV. Paired-pulse stimuli were delivered at 50 ms intervals every 10 s. Pulse duration was 0.1 ms and stimulating voltage was adjusted from 5 to 30 V to evoke a consistent response with low failure rate (1.5–1.7 times threshold).

Data analysis

Off-line analyses were performed using Clampfit 10 software (Molecular Devices). Only cells with action potentials higher than 45 mV and resting membrane potentials more negative than −40 mV were included in the analyses. All the presented data were not adjusted to 9–12 mV junction potential. For spontaneous and miniature EPSC and IPSC studies, the amplitude and inter-EPSC/IPSC intervals were analyzed using Mini Analysis software (Synaptosoft, Decatur, GA). A Kolmogorov-Smirnov test (K-S test, Clampfit 10) was used to statistically compare the preceding parameters in different conditions for individual cells. For comparisons between mean values, paired Student's *t*-tests were used (Origin 7.0). The amplitude and half-width duration of evoked EPSCs were determined by Clampfit 10, which,

Downloaded from jn.physiology.org on August 15, 2010

along with the paired-pulse ratio, were further statistically analyzed using independent *t*-test for individual cells and paired *t*-test for the comparison between mean values (Origin 7.0). Data were expressed as means± SE.

Drug application

All neuroactive agents were applied by bath superfusion. Drugs used in this study included the nonselective cholinergic receptor agonist carbachol (CAR, 50 μM), the competitive nonselective muscarinic cholinergic receptor (mAChR) antagonist atropine (ATR, 10 μM), the selective M2 AChR antagonist methoctramine (MTO, 10 μM), the selective M1 AChR antagonist pirenzepine (PRZ, 10 μM), the noncompetitive neuronal nicotinic AChR (nAChR) antagonist mecamylamine (MEC, 10 μM), the voltage-gated sodium channel blocker tetrodotoxin (TTX, 1 μM), nonselective calcium channel blocker cadium chloride ($CdCl_2$, 200 μM), the selective *N*-methyl-D-aspartate (NMDA) receptor antagonist 2-amino-5-phosphonovaleric acid (APV, 50 μM), the competitive AMPA/kainate glutamate receptor antagonist 6-cyano-7-nitroquinoxaline-2,3-dione (CNQX, 10 μM), the specific $GABA_A$ receptor antagonist gabazine (GBZ, 10 μM), and the glycine receptor antagonist strychnine (STR, 10 μM). All drugs were purchased from Sigma (St. Louis, MO), except for TTX, which was purchased from Tocris Bioscience (Ellisville, MO).

Histology

After recording, slices were fixed overnight in 4% paraformaldehyde and stored in PBS for further immunolabeling. Goat polyclonal anti-biotin conjugated to Cy5 (USbio, Swampscott, MA) was used to identify the neurobiotin in the recorded neurons. To determine the neurontransmitter phenotype of the recorded cells, mouse monoclonal anti-brain nitric oxide synthase (bNOS) antibody (Sigma) was used as primary antibody. Goat polyclonal to mouse IgG was conjugated to Cy3 (Abcam, Cambridge, MA) to label bNOS positive neurons, which is known to be co-localized with choline acetyltransferase (ChAT) in the PPN (Dun et al. 1994; Sugaya and McKinney 1994), and is considered a marker for cholinergic neurons. Cells were identified using a Nikon confocal fluorescence microscope and images were taken using the software NIS-Elements.

RESULTS

Locations of injections and recorded cells

The thalamic injection sites in this study were located in the region of the medial, mediodorsal, centromedian, and parafascicular (Pf) nuclei of the thalamus. Most injections were ~0.5 mm in diameter in a teardrop shape spreading dorsally along the injecting pipette. The recording sites were located within the PPN as determined using a ×4 objective lens before and after recording. Neurobiotin and bNOS labeling further confirmed the location of cells within the boundaries of the PPN. Sampling of recorded cells was directed throughout the wedge-shaped nucleus, from the posterior pars compacta around the superior cerebellar peduncle to the anterior tip close to the substantia nigra. No regional differences within the PPN were detected in terms of cell type or response type.

Properties of PPN thalamic projecting neurons

It is well known that the PPN sends cholinergic projections to the thalamus (Erro et al. 1999; Kha et al. 2000) and contains cholinergic, glutamatergic, and GABAergic neurons (Clements and Grant 1990; Ford et al. 1995; Wang and Morales 2009) as well as three types of electrophysiologically distinct cells (types I–III) (Kamondi et al. 1992). In this study, we specifically examined the properties of PPN neurons with efferent projections to the thalamus. Among a total of 201 retrogradely labeled PPN output neurons that were recorded, 12.4% (n = 25/201) of them showed only LTS and were classified as type I; 52.2% (n = 105/201) of them had only Ia and were classified as type II; 29.4% (n = 59/201) were classified as type III cells because they had both LTS and Ia; and in 6% (n = 12/201) of cells, neither LTS nor Ia was detected, and we named these type IV cells. Previous recordings of PPN cells at random (Kobayashi et al. 2003) showed that ~27% of cells exhibited LTS (i.e., they were either type I or III cells); in contrast, the present results indicate that PPN thalamic-projecting neurons have a higher portion of cells with LTS (41.8%). As far as neurotransmitter phenotype is concerned, 67 recorded neurons were successfully recovered and the slices were processed for neurobiotin and bNOS immunoreactivity. Among the neurobiotin-labeled cells, 45 (67.2%) were bNOS positive and 22 (32.8%) were bNOS negative (Fig. 1). This indicates that the thalamus mainly receives cholinergic input from the PPN, with some noncholinergic projections as well.

Postsynaptic responses of PPN thalamic projecting neurons to cholinergic agents

Previous intracellular recordings showed that cholinergic PPN neurons were mainly inhibited by cholinergic input (Good et al. 2007; Leonard and Llinas 1994). In this study, we specifically determined the postsynaptic responses of retrogradely labeled PPN thalamic projecting neurons, which included both cholinergic and noncholinergic cells, to adminis-

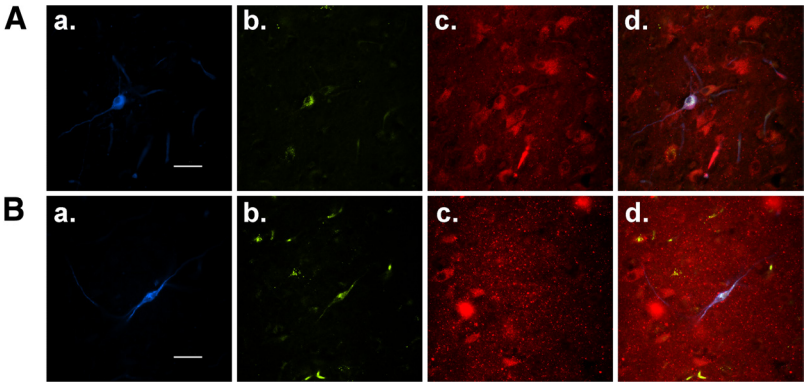

FIG. 1. Neurotransmitter phenotype of pedunculopontine nucleus (PPN) thalamic projecting neurons. *A*: a representative brain nitric oxide synthase (bNOS) labeled cholinergic PPN output neuron that was recorded using whole cell patch clamp. *a*: Cy5-conjugated neurobiotin labeling (blue); while green retrobead labeling (*b*) indicates neurons projecting to the thalamus; *c*: Cy3-labeled bNOS+ cells (red), indicative of cholinergic cells in the PPN; *d*: the overlaid view of *a*—*c*. *B*: an example of a whole cell patch clamp recorded PPN (*a*) efferent neuron (*b*), which was bNOS negative (*c*), indicating that this neuron was noncholinergic (overlay in *d*). Scale bars are 50 μm.

Downloaded from jn.physiology.org on August 15, 2010

tration of the nonselective cholinergic agonist CAR (50 μM). Among 178 PPN output neurons that were recorded at −60 mV HP, which is the average resting membrane potential of PPN neurons (Kobayashi et al. 2004), an outward current was induced by CAR in 73% (n = 130/178) of the neurons, indicating an inhibitory effect; 12.9% of them (n = 23/178) showed an inward current during application of CAR, suggesting an excitatory response; 6.7% of the cells (n = 12/178) exhibited a fast outward current followed by a slow inward current; and 7.3% (n = 13/178) of them had no response. To confirm that all these responses were due to a direct effect of CAR on the cell membrane, we blocked action potential-dependent synaptic transmission using the sodium channel blocker TTX (1 μM), or the calcium channel blocker cadmium (Cd^{2+}, 200 μM), and retested CAR on 31 CAR-inhibited, 7 CAR-excited, and 6 cells with biphasic responses. The interval between repeated applications of CAR was ~15 min. Neither of these blockers of sodium or calcium channels could eliminate the effects of CAR, suggesting that the responses observed were due to a direct activation of postsynaptic cholinergic receptors on the recorded neurons. As far as cell types are concerned (Fig. 2, *E* and *F*), it appears that those neurons showing inhibitory and biphasic cholinergic responses mainly belonged to types II and III (i.e., with Ia current) and included both cholinergic and noncholinergic cells; however, those output cells that were excited by CAR were mainly types I and III (i.e., with LTS current) and were noncholinergic.

To determine the types of cholinergic receptors that were responsible for these direct postsynaptic responses, selective cholinergic receptor antagonists were tested in the presence of TTX or Cd^{2+}. The M2 receptor has been suggested to be involved in the CAR-induced inhibitory response of cholinergic PPN neurons (Leonard and Llinas 1994); however, in the M2 knockout mouse, the M4 receptor appeared to also participate in CAR-induced hyperpolarization (Kohlmeier et al. 2007). In situ hybridization studies revealed that cholinergic cells in the PPN primarily express M2 receptors with detectable levels of M4 mRNA (Vilaro et al. 1992, 1994). However, it is not clear whether the M2 receptor is the only functionally expressed inhibitory cholinergic receptor, while the M4 receptor may only function as a compensatory reservoir of muscarinic receptors. We tested the selective M2 receptor antagonist

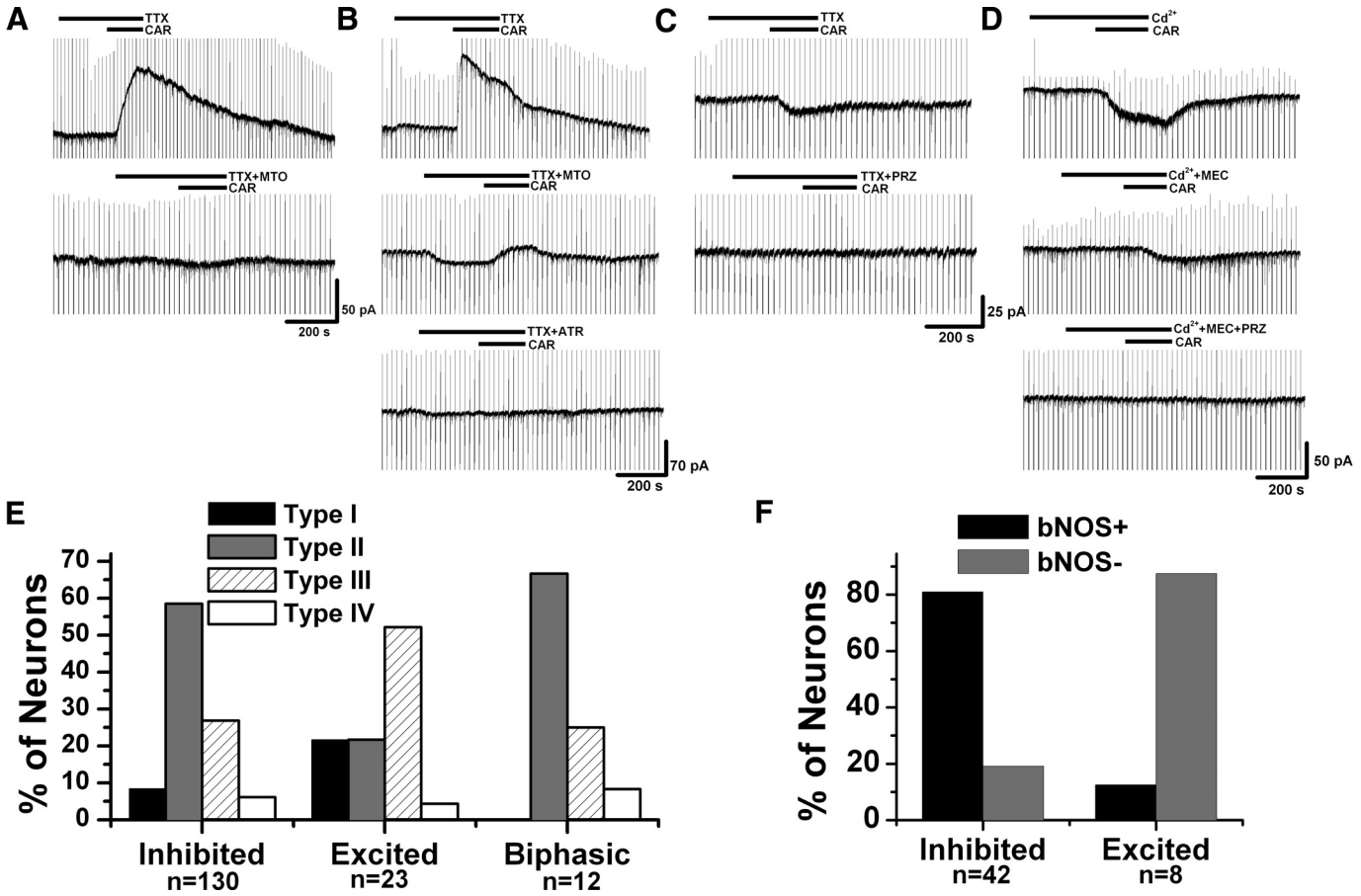

FIG. 2. Postsynaptic cholinergic responses of PPN thalamic projecting neurons. *A*: an example of a PPN output neuron showing a carbachol (CAR)-induced outward current in the presence of TTX (*top*), which was blocked by the M2 receptor antagonist methoctramine (MTO, *bottom*). *B*: in this retrogradely labeled PPN output neuron, CAR induced an outward current (*top*) that was only partially blocked by MTO (*middle*) but completely blocked by atropine (ATR, *bottom*). Note the multiple steps of outward current in the top recording, and of the inward current after addition of MTO (*middle*). *C*: a representative PPN output cell exhibiting a CAR-induced inward current (*top*), which was blocked by the M1 receptor antagonist pirenzepine (PRZ, *bottom*). *D*: an inward current was induced by CAR application in this PPN output cell in the presence of cadmium (*top*). The nicotinic AChR (nAChR) antagonist mecamylamine (MEC) did not completely block the response (*middle*), but pretreatment with MEC and PRZ blocked the CAR-induced effect (*bottom*). *E*: percentage of different types of neurons that showed inhibitory, excitatory, or biphasic cholinergic responses, respectively. *F*: group data of neurotransmitter phenotypes (cholinergic vs. noncholinergic) of neurons showing different cholinergic responses. This result suggests that cholinergic neurons tend to be inhibited and noncholinergic neurons tend to be excited by cholinergic input.

Downloaded from jn.physiology.org on August 15, 2010

methoctramine (MTO, 10 μM) on 13 PPN output cells in the presence of TTX and 11 in the presence of Cd^{2+}, respectively. MTO completely blocked the CAR-induced outward current in 6 of 13 cells in the presence of TTX and only partially blocked the current in the other 7 cells by 65 ± 9%, which were completely blocked by subsequent application of the nonselective muscarinic receptor antagonist ATR (10 μM; $n = 5$; Fig. 2, *A* and *B*). In experiments using Cd^{2+}, the outward current induced by CAR was completely blocked by MTO in 8 of 11 neurons but only partially blocked by 70 ± 7% in the other 3 cells. The amplitudes of the CAR-induced outward currents that could be completely blocked by MTO were significantly lower than those that were partially inhibited by MTO (17 ± 5 vs. 60 ± 11 pA, independent *t*-test, $P < 0.005$) suggesting the additional activation of a non-M2 receptor in the latter case. These data indicate that M2 receptors, and most probably M4 receptors as well, are involved in the inhibitory cholinergic responses in PPN thalamic projecting neurons.

With regard to the mechanisms involved in the CAR-induced inward currents, it has been reported that both muscarinic (mAChR) and nicotinic (nAChR) receptors can be involved in the cholinergic excitatory responses in the PPN (Good et al. 2007). However, it is unclear which subtype(s) of mAChRs are involved and to what extent, especially in PPN output neurons. We tested the selective M1 mAChR antagonist PRZ (10 μM) and/or the nAChR antagonist MEC (10 μM) on five cells in the presence of TTX or Cd^{2+}. PRZ completely blocked the CAR-induced inward current in three of five cells; however, in the other two cells, both PRZ and MEC were required to completely block the inward current (Fig. 2, *C* and *D*). This suggests that CAR-induced excitatory responses in PPN output neurons were due to the activation of M1 and nAChRs.

Previous studies in the thalamus (Ye et al. 2009) suggest that the biphasic cholinergic response (fast inhibition followed by slow excitation) may be due to activation of multiple types of mAChRs. In this study, however, we found that ATR completely blocked the biphasic cholinergic response in only one of the three cells tested in the presence of TTX or Cd^{2+}. In the other two cells, the CAR-induced fast outward current was successfully blocked by ATR (data not shown), while the inward current persisted; suggesting that, in the PPN, the biphasic cholinergic response may be due to activation of both mAChRs and nAChRs.

Cholinergic modulation of fast inhibitory synaptic transmission to PPN thalamic projecting neurons

Fast inhibitory synaptic transmission is mainly modulated by $GABA_A$, $GABA_C$, and glycine receptors, which belong to the ionotropic receptor family. In this study, a high Cl^- intracellular solution was used to enhance the detection of IPSCs at HP = −60 mV in the presence of AMPA/kainate and NMDA receptor blockers (CNQX 10 μM and APV 50 μM). Experiments using the selective $GABA_A$ receptor blocker GBZ (10 μM) and the glycine receptor antagonist STR (10 μM) on retrogradely labeled PPN neurons, revealed that fast inhibitory synaptic transmission to PPN thalamic projecting neurons is modulated by both $GABA_A$ and glycine receptors (Fig. 3, *A* and *B*).

The CAR effect on IPSCs was examined on 69 retrogradely labeled PPN thalamic projecting neurons. The amplitude and inter-IPSC intervals of spontaneous IPSC (sIPSCs) events detected in 20–40 s recordings in control condition with CNQX and APV, and during additional application of CAR, were statistically compared using a K-S test for individual

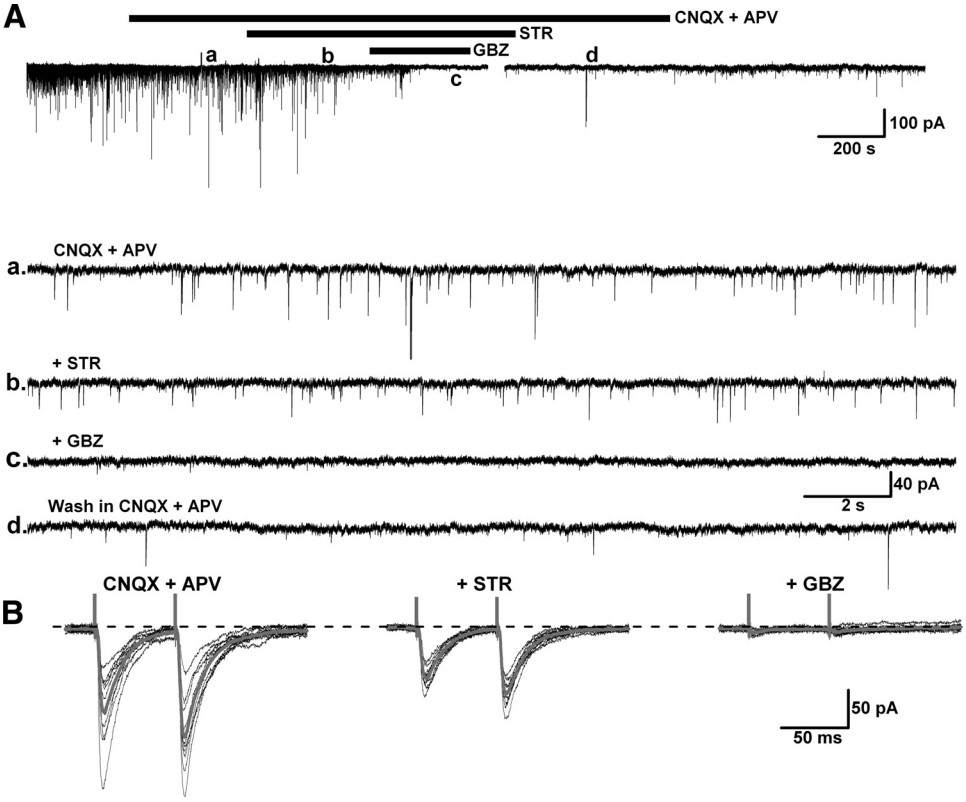

FIG. 3. Fast inhibitory innervation of PPN thalamic projecting neurons. *A*: the glycinergic receptor antagonist strychnine (STR, b) decreased spontaneous inhibitory postsynaptic currents (sIPSCs) in the presence of the AMPA/kainate receptor antagonist 6-cyano-7-nitroquinoxalene-2,3-dione (CNQX) and the *N*-methyl-D-aspartate (NMDA) receptor antagonist 2-amino-5-phosphonovaleric acid (APV, *a*), while further addition of the $GABA_A$ receptor antagonist GBZ abolished the IPSCs (*c*), which recovered after wash (*d*). *B*: the amplitude of evoked IPSCs in a PPN output neuron (*left*) was attenuated by STR (middle record) and blocked by additional application of GBZ (*right*). The gray records represent the average of 10 individual trials (black) in each condition. This result suggests that fast inhibitory synaptic transmission to PPN thalamic projecting neurons is modulated by both glycinergic and $GABA_A$ receptors.

Downloaded from jn.physiology.org on August 15, 2010

cells. Forty-five of 69 (65.2%) cells tested showed a significant decrease in the inter-IPSC intervals of sIPSCs in the presence of CAR (K-S test, $P < 0.00001$), suggesting that presynaptic GABAergic and/or glycinergic neurons were excited by CAR. The mean interevent interval decreased from 1.3 ± 0.2 s in the presence of CNQX and APV to 0.2 ± 0.03 s during CAR application ($n = 45$, paired t-test, $P < 0.001$; Fig. 4). In addition to the decrease in inter-IPSC intervals, 29 cells showed a significant increase in the amplitude of sIPSCs during CAR application from 33.4 ± 2.4 to 66.1 ± 6.6 pA ($n = 29$, paired t-test, $P < 0.001$). In the other 24 neurons, 20 of them (29%) showed no significant change in the inter-IPSC intervals during CAR application (2.6 ± 0.4 s before CAR, 2.9 ± 0.6 s during CAR; $n = 20$, paired t-test, $P = 0.41$) nor did the amplitude of sIPSCs significantly change (33.9 ± 3.1 pA before CAR, 35.5 ± 3.5 pA during CAR; $n = 20$, paired t-test, $P = 0.62$). For the other four cells (5.8%), a significant increase in the inter-IPSC intervals (K-S test, $P < 0.00001$) induced by CAR was observed from 0.8 ± 0.2 to 3 ± 0.8 s ($n = 4$, paired t-test, $P < 0.05$). There were no correlations between CAR-induced postsynaptic responses and changes in sIPSCs. Also no relationship between changes in sIPSCs and electrophysiological (types I–III) or neurotransmitter phenotype (cholinergic and noncholinergic) could be determined from our data.

Because fast inhibitory synaptic transmission to the majority of PPN thalamic-projecting neurons was enhanced by the cholinergic agonist CAR, we next focused on identifying the mechanisms of the CAR-induced increase in IPSCs. We first tested the M1 receptor antagonist, PRZ, on 11 of the 45 PPN efferent neurons that exhibited CAR-increased sIPSCs and found that PRZ successfully blocked the CAR effect on 8 of them (1.2 ± 0.3 s inter-IPSC interval in the control condition with CNQX, APV, and PRZ, and 1.3 ± 0.5 s during CAR; $n = 8$, paired t-test, $P = 0.71$; Fig. 5, *A–C*). For the other three cells, the mean inter-IPSC interval was reduced from 0.8 ± 0.3 to 0.2 ± 0.06 s after CAR application ($n = 3$, paired t-test, $P = 0.11$). No significant change in the amplitude of sIPSCs (38.4 ± 7.1 pA in the control and 39.8 ± 6.3 pA with CAR; $n = 10$, paired t-test, $P = 0.53$) was observed in 10 of these 11 cells. Considering that PRZ did not completely block the CAR-induced increases in sIPSCs and that the nAChR is another important excitatory cholinergic receptor in the PPN, we applied MEC to 12 of 45 cells showing CAR-induced increases in sIPSCs. Pretreatment with MEC abolished the CAR-induced increase in sIPSCs in only one cell; while in the majority of tested cells ($n = 11/12$), CAR still decreased the inter-IPSC interval (1.6 ± 0.5 s in the presence of CNQX, APV, and MEC, 0.2 ± 0.05 s during CAR; $n = 11$, paired t-test, $P < 0.05$; Fig. 5, *D–F*). In addition, MEC did not block the CAR-induced increase in the amplitude of sIPSCs (from 32.8 ± 2.9 to 77.7 ± 10.6 pA; $n = 6$, paired t-test, $P < 0.05$). From these data, it appears that the nAChR is not significantly, if at all, involved in the cholinergic excitation of GABAergic and/or glycinergic cells that are presynaptic to thalamic projecting neurons. We performed further experiments using ATR and found that it successfully abolished all the effects that CAR had on sIPSCs (Fig. 5, *G–I*). The mean inter-IPSC interval was 1.8 ± 0.5 s in the control condition with CNQX, APV, and ATR, and during CAR application, it was 1.7 ± 0.7 s ($n = 6$, paired t-test, $P = 0.90$). The mean amplitude of the IPSCs was 40.1 ± 9.7 and 38.2 ± 7.6 pA, respectively, in the control condition and during CAR ($n = 6$, paired t-test, $P = 0.64$). To confirm that the lack of CAR effect on sIPSCs was indeed due to blockade of cholinergic receptors and not due to receptor desensitization, we repetitively superfused CAR at 15 min intervals on nine cells and the effects were successfully replicated. The previous pharmacological data (Fig. 6, *D* and *E*), suggest that the cholinergic excitation of GABAergic and/or glycinergic neurons presynaptic to PPN

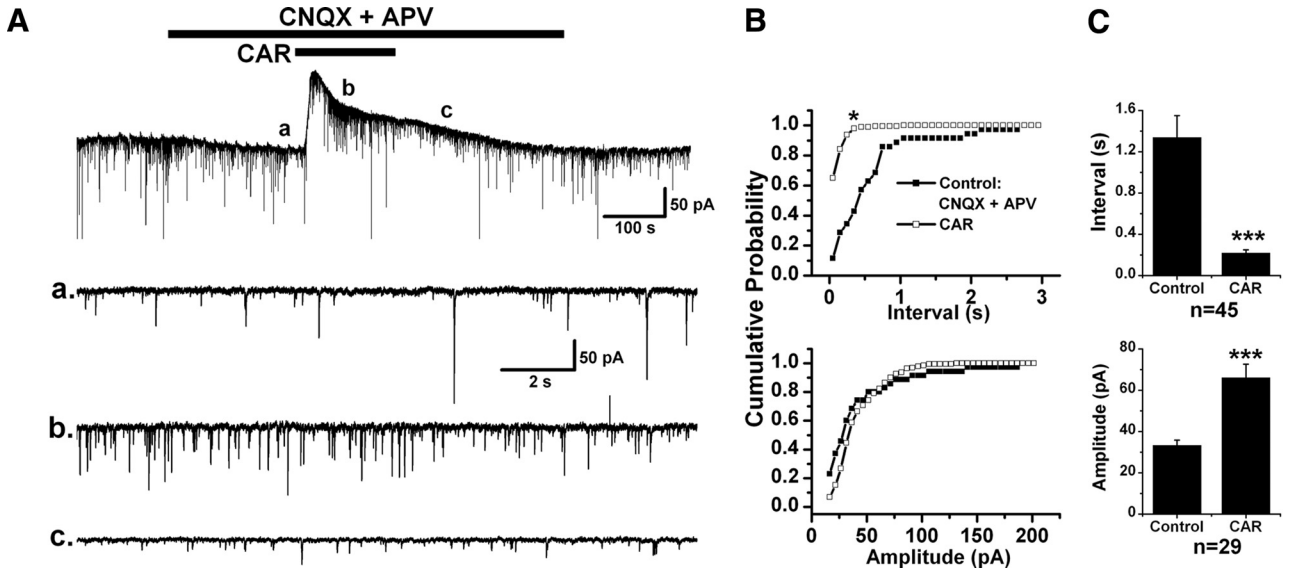

FIG. 4. Cholinergic modulation of sIPSCs in PPN thalamic projecting neurons. *A*: CAR increased the frequency of sIPSCs in a PPN output neuron that showed a CAR-induced outward current (*top*). Enlarged representative records in each condition are shown below, in records before CAR (*a*), during CAR (*b*), and after CAR (*c*). *B*: cumulative probability distributions of the inter-IPSC interval (*top*) and amplitude (*bottom*) of sIPSCs in each condition for the cell in *A* that were obtained from 20 s recording samples in each condition. A left shift of the cumulative inter-IPSC interval distribution indicates a decrease in the interval [*Kolmogorov-Smirnov (K-S) test, $P < 0.00001$; *top*]. CAR did not significantly change the amplitude of sIPSCs in this neuron (*bottom*). *C*: summary of the CAR effect on the inter-IPSC interval (*top*) and amplitude (*bottom*) of sIPSCs. In 45 tested PPN output neurons, an increase in sIPSCs frequency (*top*) and amplitude (*bottom*) was induced by CAR, implying a cholinergic excitation of presynaptic GABAergic and/or glycinergic neurons (***paired t-test, $P < 0.001$).

Downloaded from jn.physiology.org on August 15, 2010

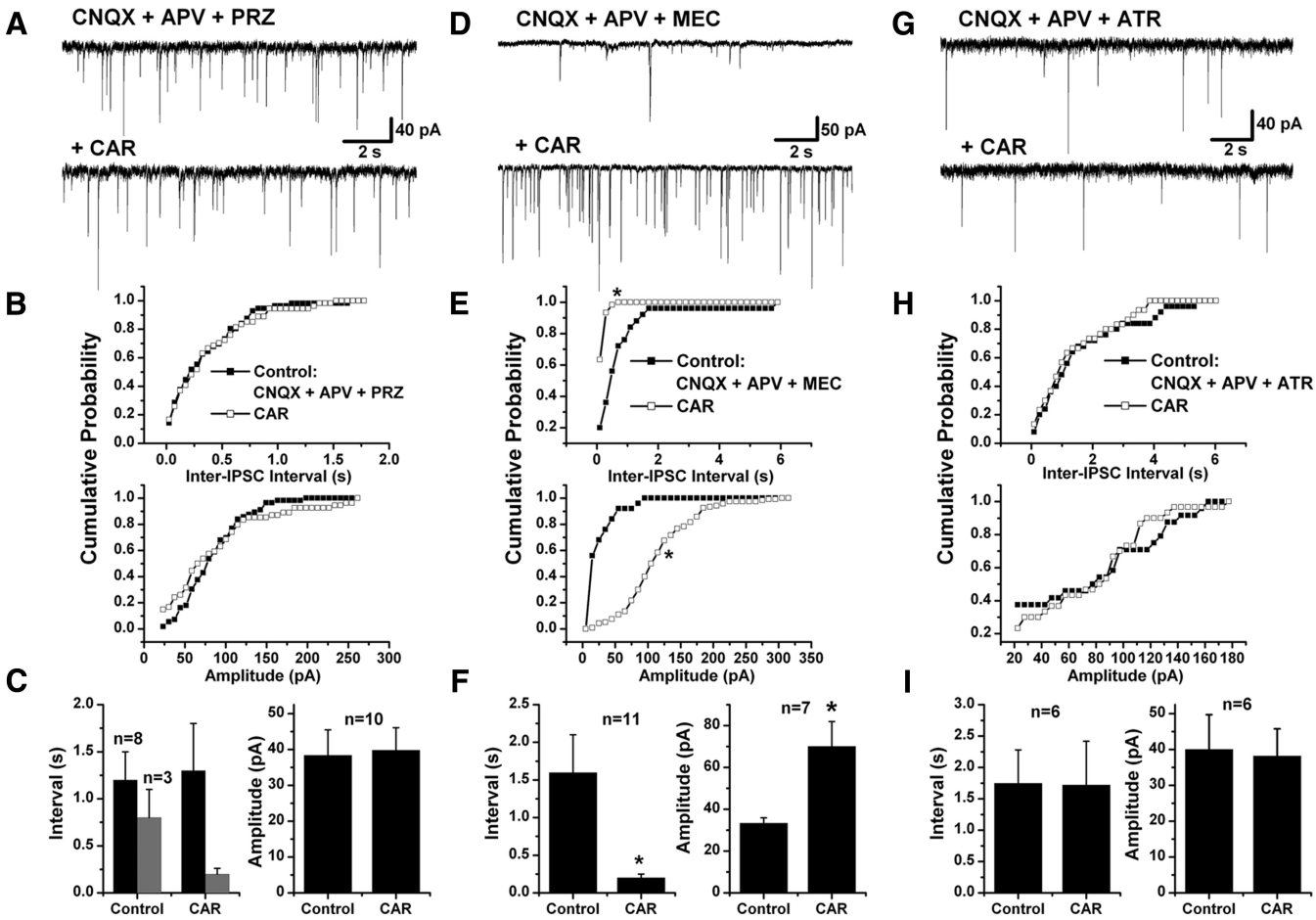

FIG. 5. Cholinergic receptor(s) responsible for the sIPSCs increase. *A, D,* and *G*: representative recordings in the presence of PRZ, MEC, and ATR, respectively, together with CNQX and APV (*top*). CAR did not change either the inter-IPSC interval or the amplitude of sIPSCs in the presence of PRZ and ATR (in *A* and *G, bottom*), while it increased sIPSCs in the presence of MEC (*D, bottom*). *B, E,* and *H*: cumulative probability distributions of inter-IPSC intervals and amplitude of sIPSCs in each condition for cells in *A, D,* and *G,* respectively, that did not change in *B* and *H* but significantly increased in *E* (*K-S test, $P < 0.00001$). *C, F,* and *I*: a summary of the effects of CAR on the inter-IPSC intervals and amplitude of sIPSCs in the presence of PRZ (*C*), MEC (*F*), and ATR (*I*) in PPN thalamic projecting neurons. It appears that the CAR-induced increase in sIPSCs was due to activation of muscarinic AChRs (mAChRs), especially M1Rs (* paired *t*-test, $P < 0.05$).

thalamic-projecting neurons is mediated mainly through activation of muscarinic receptors, especially M1Rs.

sIPSCs correspond to the sum of two types of synaptic activity. The first type of activity is TTX-sensitive and reflects the level of spontaneous firing in soma/axons of GABAergic or glycinergic neurons that are presynaptic to the recorded cells. The other type of activity is TTX-resistant and corresponds to action potential-independent spontaneous release of GABA or glycine from synaptic terminals, named miniature IPSCs (mIPSCs). A change in the frequency of mIPSCs is usually indicative of presynaptic modulation of the probability of transmitter release. To further distinguish whether the CAR-induced increase in the frequency of sIPSCs was due to activation of cholinergic receptors at presynaptic terminals, or on the soma and/or axons of GABAergic and/or glycinergic neurons, the modulation by CAR of mIPSC properties was examined in the presence of CNQX, APV, and TTX on 7 of 45 PPN thalamic-projecting neurons showing CAR-induced increase in sIPSCs. No significant change in the inter-IPSC interval of mIPSCs was observed in any of these cells (2.1 ± 0.5 s in the presence of CNQX, APV, and TTX, 2.1 ± 0.5 s after addition of CAR; $n = 7$, paired *t*-test, $P = 0.91$; Fig. 6, *A–C*). Furthermore, no change in the amplitude of mIPSCs was detected in any of these seven cells (50.4 ± 9.3 pA before CAR, 45.1 ± 5.8 pA after CAR; $n = 7$, paired *t*-test, $P = 0.25$). Taken together, these data suggest that the somata rather than the synaptic terminals of GABAergic and/or glycinergic neurons are the main sites of modulation by cholinergic agents.

Cholinergic modulation of fast excitatory synaptic transmission to PPN thalamic projecting neurons

Glutamate ionotropic receptors (NMDA, AMPA, and kainate) are responsible for fast excitatory synaptic transmission in the CNS. However, under our experimental conditions (using 1.2 mM extracellular Mg^{2+}), fast synaptic excitatory transmission, manifested as EPSCs, are mainly driven by activation of AMPA and/or kainate receptors at HP = −60 or −70 mV because the NMDA receptor remains mostly inactivated at this HP. As expected, the NMDA receptor antagonist, APV, did not significantly affect spontaneous or evoked EPSCs in the presence of GBZ and STR; however, these EPSCs were almost completely (87.5 ± 0.3%) blocked by the AMPA/kainate receptor antagonist CNQX (Fig. 7).

Downloaded from jn.physiology.org on August 15, 2010

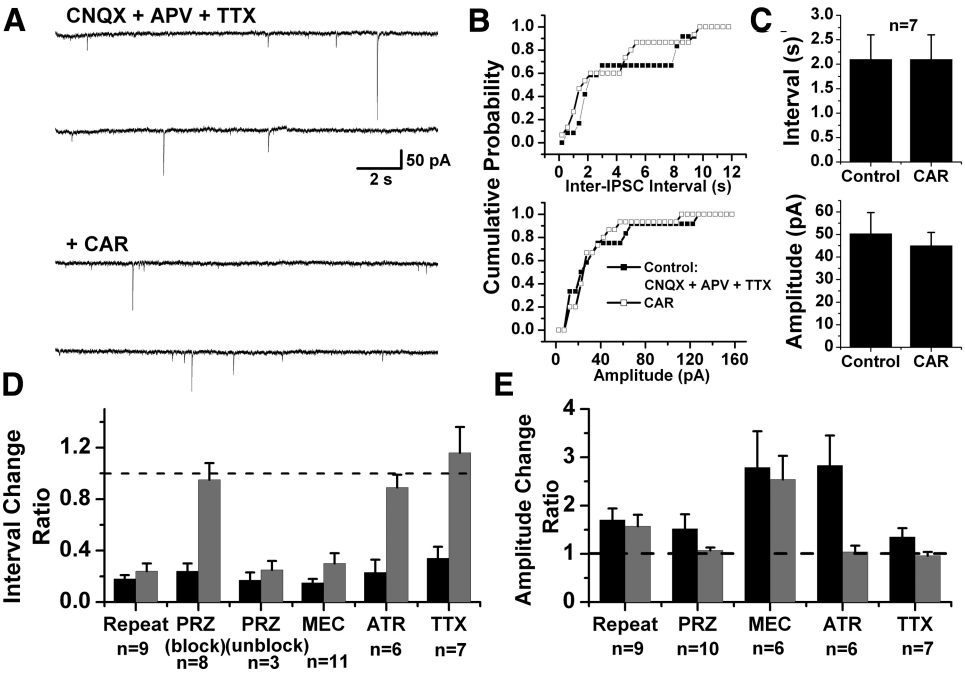

FIG. 6. Cholinergic modulation of mIPSCs in PPN thalamic projecting neurons. *A*: representative recordings in the presence of CNQX, APV, and TTX (*top 2 records*), and after addition of CAR (*bottom 2 records*). Two records are shown due to the low frequency of events. *B*: cumulative distributions of inter-IPSC interval and amplitude of mIPSCs for the cell in *A* that were obtained from 30 s recording samples. *C*: summary of CAR effects on mIPSCs in PPN thalamic projecting neurons. CAR did not significantly change inter-IPSC intervals (*top*) or amplitude (*bottom*) of mIPSCs. *D* and *E*: summaries of the effects of cholinergic antagonists and TTX on CAR-induced increases in sIPSCs. The interval/amplitude change ratio was obtained by using the inter-IPSC interval or amplitude of IPSCs during CAR application divided by that obtained in the control condition with only CNQX and APV or in the presence of antagonists. ■, the change in IPSCs after the 1st CAR application; ▨, the 2nd CAR response, which was obtained in the presence of antagonists or TTX.

Cholinergic modulation of spontaneous EPSCs (sEPSCs) was determined following application of CAR to 65 retrogradely labeled PPN neurons in the presence of GBZ and STR at a HP = −60 mV. A significant decrease in the inter-EPSC interval was produced in 43 of these cells (66.2%) after analyzing 20–40 s data segments before and during CAR application (K-S test, $P < 0.00001$). The mean inter-EPSC interval decreased from 0.8 ± 0.1 to 0.1 ± 0.02 s after CAR ($n = 43$, paired *t*-test, $P < 0.001$; Fig. 8). In conjunction with the reduction in sEPSC interval, a significant increase in the amplitude of sEPSCs was produced by CAR in 21 of the 43 cells (from 15.4 ± 0.9 to 21.5 ± 1.4 pA, $n = 21$, paired *t*-test, $P < 0.001$; Fig. 8). Among the other 22 neurons, 16 of them (24.6%) showed no significant change in the inter-EPSC inter-

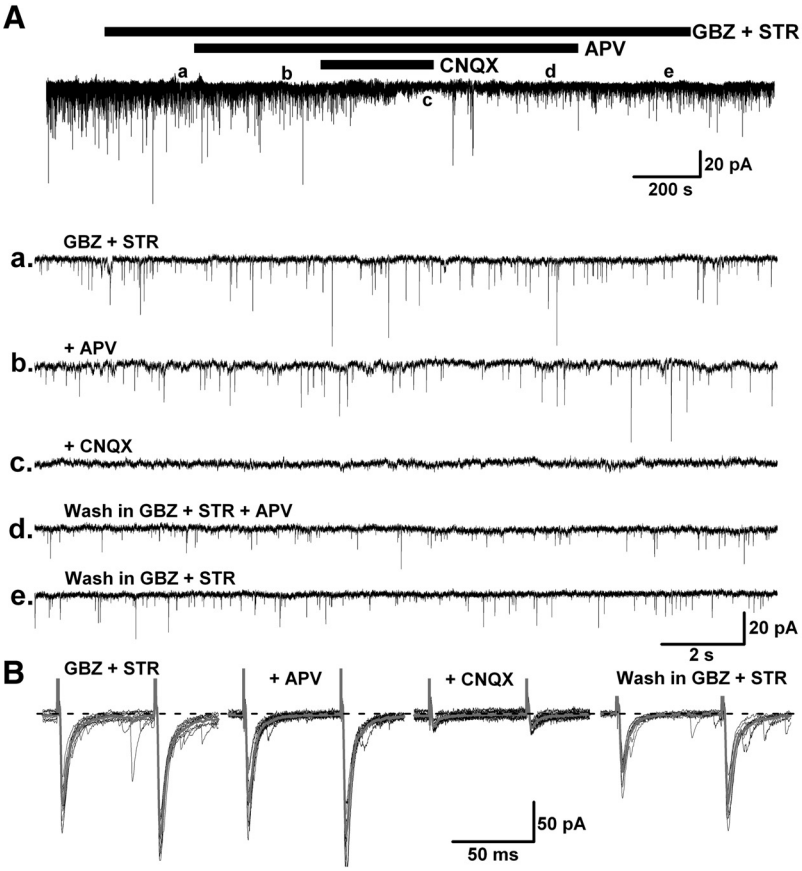

FIG. 7. Fast excitatory synaptic transmission on PPN thalamic projecting neurons. *A*: the frequency of spontaneous excitatory PSCs (EPSCs) recorded in the presence of GBZ and STR (*a*) was not significantly changed after APV application (*b*) but was abolished by CNQX (*c*) and recovered after wash (*d* and *e*). *B*: the amplitude of evoked EPSCs in a PPN output neuron (*1st record*) was not significantly attenuated by APV (*2nd record*) but was blocked by CNQX (*3rd record*), which recovered after washing in GBZ and STR (*4th record*). Gray records represent the average of 10 individual trials (black records) in each condition. This result indicates that fast excitatory synaptic transmission to PPN thalamic projecting neurons was mainly modulated by AMPA/kainate receptors in our experimental conditions.

Downloaded from jn.physiology.org on August 15, 2010

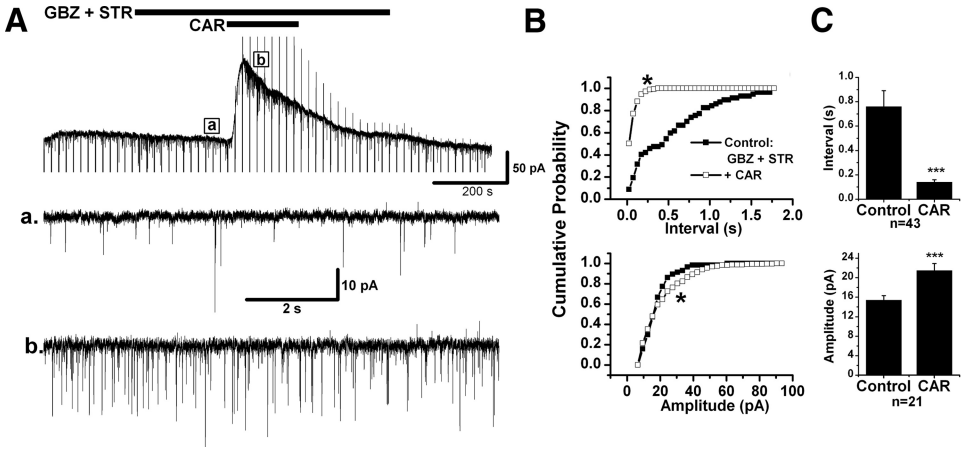

FIG. 8. Cholinergic modulation of spontaneous EPSCs (sEPSCs) in PPN thalamic projecting neurons. *A*: CAR increased the frequency of sEPSCs in a PPN output neuron that showed a CAR-induced outward current. Enlarged representative records in each condition are shown below, records before (*a*) and during CAR (*b*). *B*: cumulative probability distributions of the inter-EPSC interval (*top*) and amplitude (*bottom*) of sEPSCs in each condition for the cell shown in *A* that were obtained from 20 s recording samples in each condition. A left shift in the cumulative inter-EPSC interval distribution indicates a decrease in the interval (*top*). A right shift of the cumulative amplitude distribution (*bottom*) suggests a significant increase in sEPSC amplitude by CAR in this neuron (*K-S test, $P < 0.00001$). *C*: summary of the CAR effects on the inter-EPSC interval and amplitude of sEPSCs. Forty-three output cells showed a significant decrease in interval, while 21 cells showed a significant increase in amplitude after CAR application, suggesting that the majority of presynaptic glutamatergic neurons projecting to PPN output neurons are excited by this cholinergic agent (***paired *t*-test, $P < 0.001$).

val during CAR application (0.7 ± 0.1 s before CAR, 0.7 ± 0.1 s during CAR; $n = 16$, paired *t*-test, $P = 0.37$) nor did the amplitude of sEPSCs significantly change (15.0 ± 1.0 pA before CAR, 15.5 ± 1.9 pA during CAR; $n = 16$, paired *t*-test, $P = 0.62$). For the other six cells (9.2%), CAR significantly increased in the mean inter-EPSC interval from 0.4 ± 0.1 to 1.0 ± 0.2 s ($n = 6$, paired *t*-test, $P < 0.01$). Similar to the CAR effects on presynaptic GABAergic and/or glycinergic neurons, it seems that the majority of glutamatergic neurons presynaptic to PPN thalamic projecting cells was also excited by CAR (Fig. 8, *D–F*), while no direct relationship was found between changes in sEPSCs and CAR-induced postsynaptic responses or cell type.

Excitatory cholinergic receptor antagonists were tested on those neurons showing CAR-induced increase in sEPSCs to determine the specific receptors that were responsible for the excitation of presynaptic glutamatergic neurons. PRZ successfully abolished the CAR effect in seven of eight tested cells (1.4 ± 0.6 s inter-EPSC interval in the control condition with GBZ, STR, and PRZ, 1.2 ± 0.5 s during addition of CAR; $n = 7$, paired *t*-test, $P = 0.42$; Fig. 9). After pretreatment with MEC in the presence of GBZ and STR, CAR still significantly reduced the inter-EPSC interval (K-S test, $P < 0.00001$) in seven of eight cells, and the mean value decreased from 1.1 ± 0.5 to 0.2 ± 0.06 s ($n = 7$, paired *t*-test, $P = 0.09$). In experiments using ATR, no significant change was observed in the inter-EPSC interval after CAR application (0.8 ± 0.3 s before CAR, 0.8 ± 0.2 s during CAR; $n = 6$, paired *t*-test, $P = 0.91$). It thus appears that glutamatergic neurons presynaptic to PPN output neurons are excited by CAR mainly through M1 receptors. The effects of these antagonists are shown in Fig. 10, *D* and *E*.

In the presence of GBZ, STR, and TTX, CAR effects on miniature EPSCs (mEPSCs) were tested in seven neurons that exhibited CAR-induced decreases in sEPSC interval in the absence of TTX. Even though only one cell responded by a significant increase in inter-mEPSC interval (K-S test, $P < 0.00001$), six neurons showed a nonsignificant increase in the inter-mEPSC interval during CAR application (0.8 ± 0.4 s before CAR, 1.2 ± 0.5 s in the presence of CAR, $n = 6$, paired *t*-test, $P = 0.08$; Fig. 10, *A–C*). CAR produced no significant change in the amplitude of mEPSCs (14.1 ± 1.8 pA in the control, 14.6 ± 1.6 pA during CAR; $n = 7$, paired *t*-test, $P = 0.28$). The CAR-induced increase in the mean mEPSC interval was blocked by pretreatment with the M2 receptor antagonist MTO (1.1 ± 0.7 s inter-mEPSC interval in the control with GBZ, STR, TTX, and MTO, 0.9 ± 0.4 s during CAR; $n = 4$, paired *t*-test, $P = 0.54$; data not shown). These data suggest the possible presence of M2 receptors at the synaptic terminals of glutamatergic neurons that are presynaptic to PPN thalamic projecting neurons.

To further test for the presence of presynaptic M2 receptors, evoked EPSC experiments were conducted. A bipolar stimulating electrode was placed in the PPN, and paired-pulse eEPSCs were recorded in retrogradely-labeled PPN neurons 50–200 μm away at a HP = −70 mV. The effects of CAR on the amplitude, half-width duration, and paired-pulse ratio (PPR, amplitude of the second eEPSC divided by the 1st) of eEPSCs were determined in the presence of GBZ and STR. Comparison of eEPSCs before and during application of CAR on individual cells, using 10 events in each condition (independent *t*-test), revealed that among 20 PPN output neurons, 17 cells showed a significant decrease in the amplitude of eEPSCs (168.3 ± 19.8 pA in the control, 90.3 ± 13.8 pA during CAR; $n = 17$, paired *t*-test, $P < 0.001$; Fig. 11, *A–C*). In association with the amplitude decrease, 14 cells demonstrated a significant decrease in eEPSC half-width duration (from 8.1 ± 0.8 to 6.3 ± 0.7 ms; $n = 14$, paired *t*-test, $P < 0.005$). Moreover, the mean PPR increased from 1.5 ± 0.1 to 1.7 ± 0.2 after addition of CAR ($n = 17$, paired *t*-test, $P < 0.05$). We further tested MTO on five neurons exhibiting CAR-induced decreases in eEPSCs and found that the CAR effects were abolished in four of them. The other neuron was excluded from the analysis because it showed a continuous rundown in the amplitude of eEPSCs during CAR application. The mean amplitude of eEPSCs was 124.3 ± 47.6 pA in the control condition with

Downloaded from jn.physiology.org on August 15, 2010

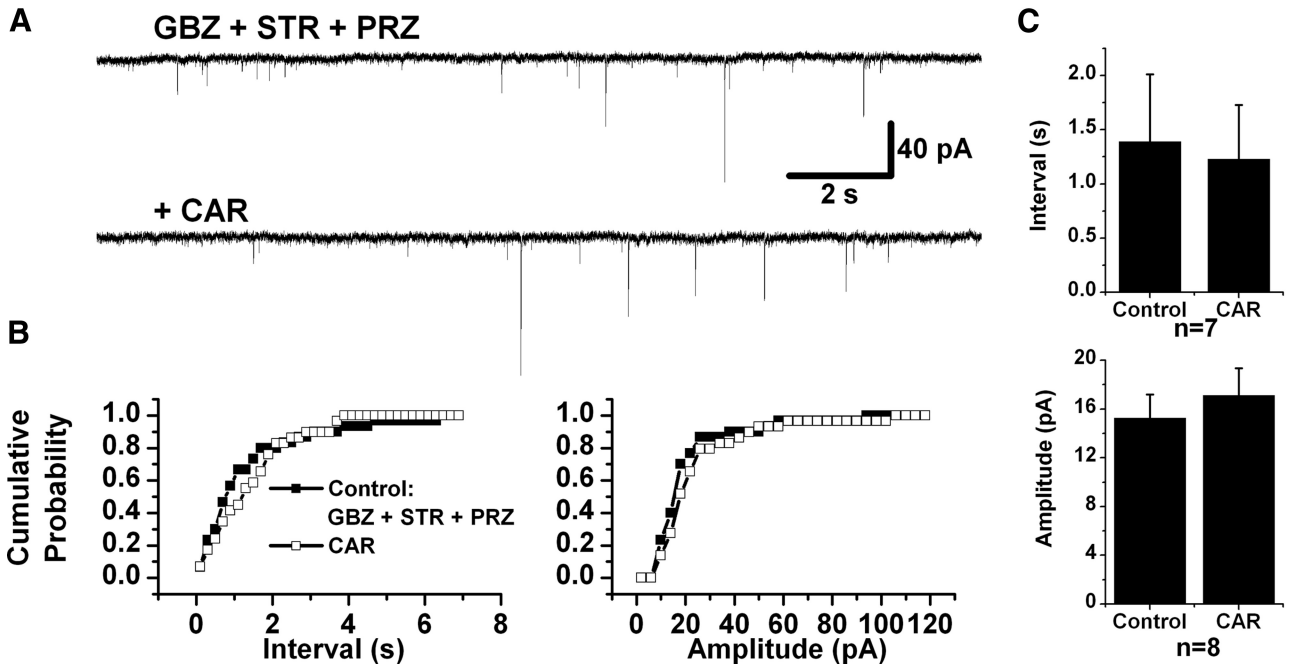

FIG. 9. Cholinergic receptor(s) responsible for the sEPSCs increase. *A*: representative recordings in the presence of GBZ, STR, and PRZ (*top*), and after addition of CAR (*bottom*), did not show a change in sEPSCs. *B*: cumulative distributions of inter-EPSC interval (*left*) and amplitude (*right*) of sEPSCs in each condition for recordings in *A*. Samples were taken from 20 s recordings in each condition. *C*: summary of effects of CAR on sEPSCs in the presence of PRZ. It appears that PRZ successfully abolished the CAR-induced increase in sEPSCs, indicating that presynaptic glutamatergic neurons were mainly activated by cholinergic input through M1 receptors.

GBZ, STR, and MTO, and 103.1 ± 41.0 pA during additional CAR application ($n = 4$, paired *t*-test, $P = 0.19$); the mean half-width duration was 8.2 ± 2.0 ms in control and 7.4 ± 2.4 ms during CAR ($P = 0.47$); and the mean PPR was 1.6 ± 0.1 and 2.1 ± 0.6 in control and during CAR, respectively ($P = 0.50$; Fig. 11, *D* and *E*).

Considering that the change in half-width duration of eEPSCs may indicate a modulation of the conductance or the kinetic properties of postsynaptic ionotropic glutamate receptor channels, we suspected that a change in membrane input resistance, caused by CAR, may have altered the kinetic properties of AMPA/kainate receptors. Thus we replaced Na_2GTP in the pipette solution with 1 mM GDP-β-S to block G protein coupled receptors in the recorded cells and prevent CAR from activating postsynaptic muscarinic cholinergic receptors, which mediate the decrease in membrane input resistance (Heister et al. 2009; Ye et al. 2009). As expected, five retrogradely labeled PPN cells recorded under these conditions did not show significant changes in the half-width duration of eEPSCs after CAR addition (4.1 ± 0.7 ms in the presence of GBZ and STR, 4.2 ± 0.8 ms after CAR application; $n = 5$, paired *t*-test, $P = 0.69$); however, a significant decrease in the amplitude of eEPSCs (from 245.3 ± 57.5 to 120.5 ± 34.2 pA; $P < 0.01$), and an increase in the PPR (from 1.4 ± 0.1 to 1.8 ± 0.1; $P < 0.005$) were still produced (Fig. 11, *F* and *G*). Therefore the previously observed CAR-induced decrease in eEPSC half-width was most likely due to postsynaptic mechanisms that may involve a shunting effect caused by a membrane input resistance decrease in response to CAR. Taken together, the mEPSC and eEPSC data suggest the presence of M2 receptors at the presynaptic terminals of glutamatergic neurons that provide excitatory inputs to PPN thalamic projecting neurons.

DISCUSSION

This study determined that *1*) not only cholinergic PPN neurons but also noncholinergic PPN cells send efferent projections to the thalamus, but they may respond differently to cholinergic inputs, *2*) GABAergic and/or glycinergic neurons that are presynaptic to PPN output neurons appeared to be excited by cholinergic agonists, mainly through the activation of M1 receptors located on their soma and/or axons, and *3*) glutamatergic neurons presynaptic to PPN efferent neurons were likely to be excited mainly via activation of M1 receptors on their soma and/or axons, however, their synaptic terminals had inhibitory M2 receptors. These results are summarized in Fig. 12.

Postsynaptic cholinergic responses of PPN thalamic projecting neurons and their properties

It was previously assumed that PPN neurons with efferent projections to the thalamus are mainly cholinergic, while noncholinergic PPN cells preferentially project to the basal ganglia (Mena-Segovia et al. 2008). Our retrograde labeling experiment showed that both cholinergic and noncholinergic PPN neurons send efferent projections to the thalamus. However, it remains to be determined whether these noncholinergic thalamic projecting neurons are GABAergic, glutamatergic, or both. In terms of electrophysiological properties, ~70% of PPN neurons were categorized as type II cells with only Ia and 27% of cells were type I or III with LTS in previous sharp intracellular recording studies (Kobayashi et al. 2003). Our present study suggests that retrogradely labeled thalamic projecting PPN neurons consist of a higher proportion of neurons with LTS (~42%). The presence of LTS promotes the generation of bursts of action potentials, which underlie the firing patterns observed in PGO-on peribrachial (PB) and LDT neu-

Downloaded from jn.physiology.org on August 15, 2010

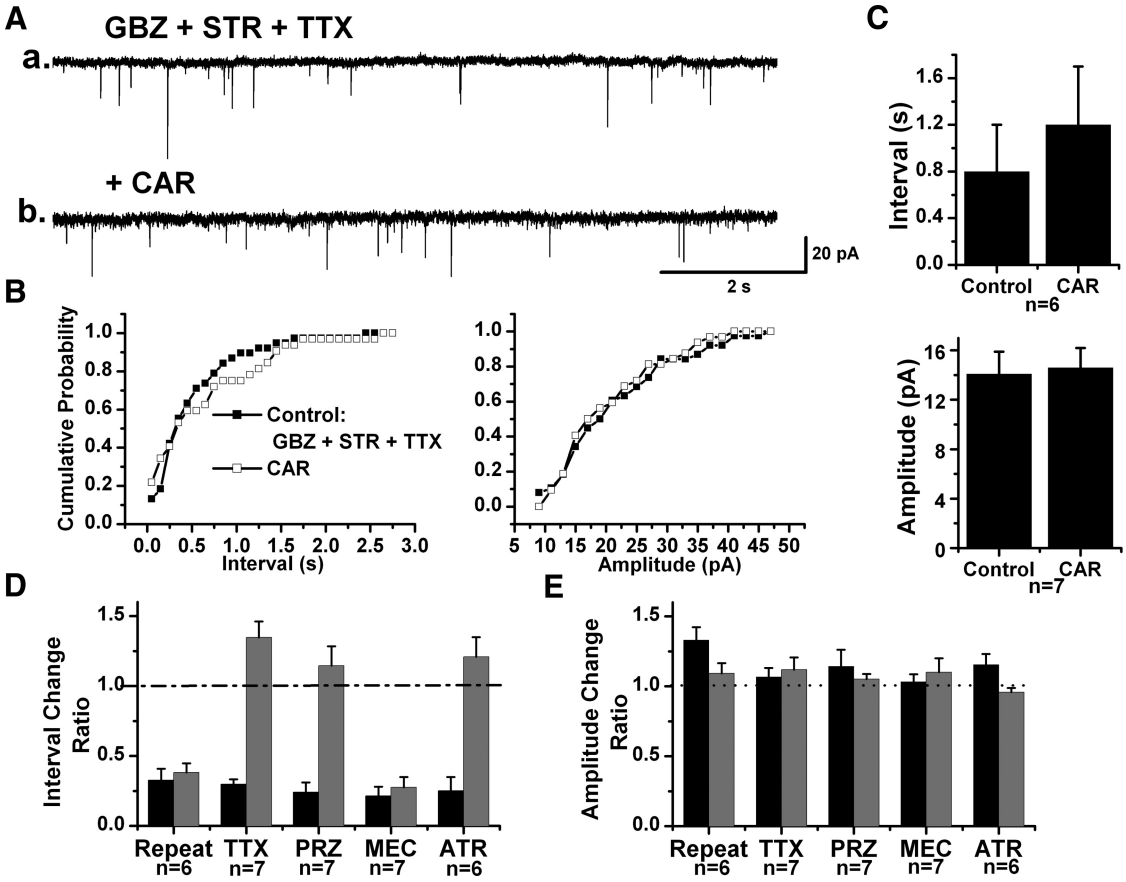

FIG. 10. Cholinergic modulation of mEPSCs in PPN thalamic projecting neurons. *A*: in the presence of TTX, no significant change in the frequency of mEPSCs was observed in this PPN output neuron. *a* and *b*: representative recordings in each condition. *B*: cumulative probability distributions of the inter-EPSC interval and amplitude of mEPSCs in each condition for the recording in *A*. Events were from 20 s recording samples in each condition. A slight right shift in the cumulative distribution of intervals indicates a nonsignificant decrease in the frequency of mEPSCs (*left*). CAR did not significantly change the amplitude of mEPSCs in this output neuron (*right*). *C*: summary of the CAR effect on the inter-EPSC interval and amplitude of mEPSCs. A nonsignificant increase (P = 0.08) was evident in the mEPSCs interval. *D* and *E*: summaries of the effects of cholinergic antagonists and TTX on CAR-induced increased sEPSCs. The interval/amplitude change ratio was obtained by using inter-EPSC interval or amplitude of EPSCs during CAR application divided by that in the control condition with only GBZ and STR or plus antagonists. ■, the change of EPSCs after the 1st CAR application; ▤, the 2nd CAR application, which was in the presence of antagonists or TTX.

rons (Steriade et al. 1990). Moreover, when these neurons are depolarized, they are more likely to discharge with high-frequency spike bursts. Such properties may enable PPN neurons to fire at fairly high frequencies, including gamma frequency (unpublished data).

A number of reports have described the postsynaptic cholinergic responses of PPN neurons. Both nAChR- and mAChR-mediated excitation and mAChR-mediated inhibition were observed in intracellularly recorded PPN neurons (Good et al. 2007). Cholinergic PPN neurons were inhibited by activation of M2 receptors via opening of inwardly rectifying potassium channels (Leonard and Llinas 1994). Our current results extend the latter study specifically to PPN thalamic projecting neurons because this may be an essential pathway that the PPN employs to promote waking and REM sleep. Direct postsynaptic cholinergic responses of PPN neurons were determined in the presence of TTX or Cd^{2+}, which are used conventionally to block action potential-dependent presynaptic neurotransmitter release. Our study confirmed that cholinergic PPN output neurons are predominantly inhibited by cholinergic agonists (Good et al. 2007; Leonard and Llinas 1994) but not only through activation of M2 receptors because M4 receptors might be involved as well. This is consistent with the findings in either M2- or M4- transgenic mice, in which knockout of either one of these two receptors was unable to diminish the CAR-induced inhibitory response; however, it was completely abolished in M2 and M4 double knockout mice (Kohlmeier et al. 2007). In situ hybridization experiments also revealed high levels of M2 receptor mRNA, and detectable levels of M4 mRNA, in cholinergic PPN neurons (Vilaro et al. 1992, 1994). Our present study demonstrated that noncholinergic PPN output neurons can be either excited via activation of M1 and/or nAChR or inhibited by M2 and/or M4 receptors. Further investigation is required to identify whether GABAergic and glutamatergic neurons have differential responses to cholinergic agonists. In addition, there may be a small population of output neurons that have both mAChRs and nAChRs. This is supported by our finding that the biphasic response recorded in the PPN was not completely abolished by the nonspecific mAChR antagonist ATR. This result is in contrast to what we reported in the thalamus (Pf), where ATR completely blocked the biphasic CAR-induced response (Ye et al. 2009).

Downloaded from jn.physiology.org on August 15, 2010

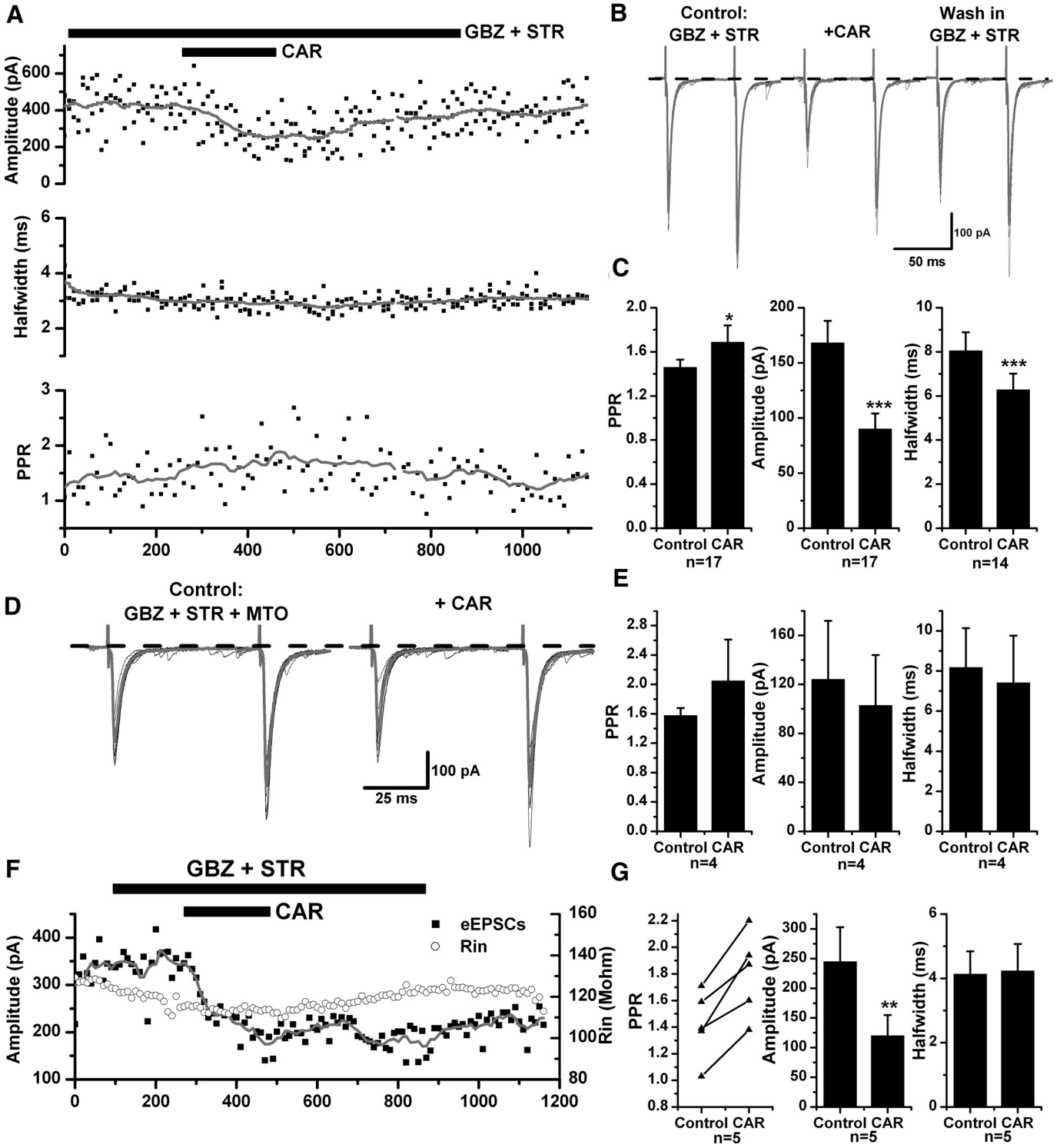

FIG. 11. Cholinergic modulation of evoked EPSCs in PPN thalamic projecting neurons. *A*: in the presence of GBZ and STR, CAR decreased the amplitude of evoked EPSCs in a PPN output neuron, which recovered after washing in GBZ and STR. The gray line was obtained using a smoothing average of 20 adjacent points (*top*). No significant change in the half-width duration was induced by CAR in this neuron (*middle*), while a significant increase in the PPR was also observed (*bottom*). *B*: average of 5 evoked EPSCs in control (GBZ and STR, *left*), in the presence of CAR (*middle*), and after washing in GBZ and STR (*right*) for the cell shown in *A*. Note the change in both amplitude and PPR. *C*: the average change of PPR (*left*), amplitude (*middle*),and half-width duration (*right*) of eEPSCs before and after CAR application. CAR significantly decreased the amplitude of eEPSCs in 17 output cells tested. *D*: after pretreatment with MTO (*left*), CAR failed to change the amplitude of eEPSC (*right*) in the same cell shown in *A*. Gray records are the average of 10 events in each condition. *E*: a summary of the effects of CAR on eEPSCs in the presence of MTO, which successfully abolished the CAR-induced decrease in their amplitude. *F*: a representative PPN output neuron recorded using GDP-β-S in the pipette solution. In this recording, CAR still significantly decreased the amplitude of eEPSCs (■) and increased the PPR, without changing the membrane input resistance (R_{in}, ○) half-width duration of eEPSCs. *G*: a summary of the effects of CAR on eEPSCs in the experiment using GDP-β-S, i.e., increased PPR (*left*), decreased amplitude (*middle*), and no change in half-width duration (*right*) (*** paired *t*-test, $P < 0.001$; ** $P < 0.01$; * $P < 0.05$).

Downloaded from jn.physiology.org on August 15, 2010

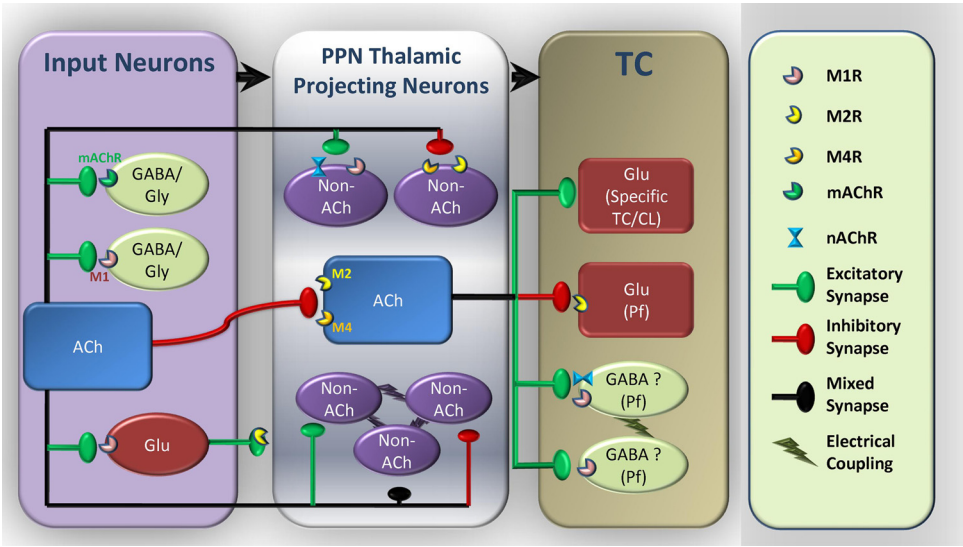

FIG. 12. Diagram of the cholinergic modulation of PPN thalamic projecting neurons and thalamocortical (TC) parafascicular (Pf) neurons. Cholinergic afferents originating from LDT and PPN predominantly inhibit cholinergic thalamic projecting PPN neurons through activation of M2 and probably M4 receptors as well (this study). Noncholinergic (GABAergic and/or glutamatergic) PPN output neurons can be either excited via M1 and nAChR or inhibited via M2 and M4 receptors (this study). Some of PPN thalamic projecting neurons are electrically coupled (Garcia-Rill et al. 2007), presumably between noncholinergic neurons. These electrically coupled neurons can be either excited or inhibited by cholinergic input (Ye et al. 2009). GABAergic and/or glycinergic neurons presynaptic to PPN thalamic projecting neurons are excited through activation of muscarinic receptors, mainly M1Rs (this study). Glutamatergic neurons presynaptic to PPN thalamic projecting neurons are excited mainly due to activation of M1 receptors, while there are some M2 receptors located at the synaptic terminals (this study). Glutamatergic Pf neurons are mainly inhibited by cholinergic input, mostly from the PPN, through activation of M2 receptors (Ye et al. 2009). However, most other TC neurons are predominantly excited by cholinergic input (Curro Dossi et al. 1991; McCormick 1992; McCormick and Prince 1987; Zhu and Uhlrich 1998). There may be some electrically coupled gabaergic interneurons in the Pf (Garcia-Rill et al. 2007), which are excited by cholinergic input via M1 and nAChR receptors, while M3 and M5 receptors are probably involved as well (Ye et al. 2009). These detailed interactions between different populations of neurons in the cholinergic arm of the reticular activating system help us understand the cellular mechanisms involved in the regulation of sleep-wake cycles.

Cholinergic modulation of fast inhibitory and excitatory transmission to PPN thalamic projecting neurons

GABAergic innervation from the substantia nigra and other sources to the PPN has been established (Granata and Kitai 1991; Saitoh et al. 2003). However, our study demonstrated that, in addition to GABAergic inputs, PPN neurons also receive glycinergic inhibitory fast synaptic inputs the origin of which has yet to be determined. This is in line with previous immunohistochemical reports of the presence of glycinergic receptors in the PPN (Fort et al. 1993; Mineff et al. 1998). Moreover we determined that fast inhibitory synaptic transmission to PPN thalamic-projecting neurons was predominantly enhanced by cholinergic agents. However, further studies are required to determine whether one or both presynaptic glycinergic and GABAergic neurons are affected by cholinergic input. Our data indicate that the potentiating effect of cholinergic agents on sIPSCs occur mainly via activation of M1 receptors located on the soma/axons of presynaptic inhibitory neurons. It should be noted, however, that in 29% (n = 20/69) of recorded output neurons, CAR did not induce significant changes in the frequency of sIPSCs. This lack of effect of CAR could occur because neurons presynaptic to the recorded cells are likely to be truncated in the slice preparation. Neurons exhibiting relatively higher frequency of sIPSC in control conditions are likely to receive more viable inputs from a larger number of inhibitory interneurons located within the slice. This possibility is supported by the finding that neurons showing no CAR-induced change in sIPSCs had, in control conditions, remarkably higher inter-IPSC intervals (i.e., lower IPSC frequency) than those showing a CAR-induced increase in sIPSCs (2.6 ± 0.4 vs. 1.3 ± 0.2 s, independent t-test, $P < 0.05$). However, the possibility that cholinergic agents differentially affect distinct groups of inhibitory presynaptic neurons should not be excluded, especially because a significant CAR-induced decrease in the frequency of sIPSCs was found in four cells.

Cholinergic modulation of fast excitatory synaptic transmission in PPN thalamic projecting neurons appears more complicated than its modulation of inhibitory transmission. Cholinergic agents seem to have differential effects on presynaptic glutamatergic neurons. Although the enhancing effect is predominant, 24.6% of cells showed no change and 9.2% had decreased frequency of spontaneous EPSCs during CAR application. Unlike sIPSCs, cells with different cholinergic responses of sEPSCs had very similar frequency in the control condition (0.8 ± 0.1 s inter-EPSC interval vs. 0.7 ± 0.1 s; P = 0.60). Therefore it is unlikely that the differential effects of CAR on EPSCs were due to the loss of glutamatergic inputs. It appears that the cholinergic receptors located on the soma of presynaptic glutamatergic neurons, as well as those located on the presynaptic terminals in contact with PPN neurons, are involved in the modulation of glutamate release. The blockade of the CAR-induced increase in the frequency of sEPSCs by PRZ indicates that presynaptic glutamatergic neurons are excited by the activation of M1 receptors on their soma/axons. However, the nonsignificant decrease in the frequency of mEPSCs, and the decrease in the amplitude of eEPSCs, along with the change in the PPR, were all abolished by MTO. This result suggests the presence of M2 receptors on the presynaptic terminals of glutamatergic neurons. It may be difficult to estimate the net cholinergic effect on PPN neurons assuming

Downloaded from jn.physiology.org on August 15, 2010

that both inhibitory and excitatory cholinergic receptors may be located on the same presynaptic glutamatergic neurons, while inhibitory cholinergic receptors are located postsynaptically on the majority of PPN output neurons. The net effect of cholinergic input might depend on where it is released and at what concentration. A local increase in acetylcholine concentration would activate M2 receptors at synaptic terminals and decrease the probability of glutamate release. However, a widespread release of acetylcholine would activate somatic M1 receptors on excitatory interneurons, which would generate action potentials, leading to additional glutamate release that may overwhelm the presynaptic inhibitory M2 effect.

Although our study revealed that cholinergic agonists predominantly enhance fast inhibitory and excitatory synaptic transmission, the origins of these GABAergic, glycinergic, and glutamatergic inputs remain to be identified. A recent report showed that noncholinergic PPN neurons do not appear to give rise to many local collaterals (Mena-Segovia et al. 2008). If this is the case, then these inputs originate more likely from other sources, which could also explain why cholinergic agents paradoxically enhance both inhibitory and excitatory inputs to PPN output neurons. GABAergic and glycinergic inhibitory and glutamatergic excitatory inputs may recruit different pathways or be active during different functional states. It is also possible that PPN neurons projecting to different targets in the thalamus are differentially modulated by cholinergic agents, especially when we consider recent reports showing a difference between PPN inputs to the Pf versus specific thalamocortical neurons (Beatty et al. 2009; Lacey et al. 2007; Phelan et al. 2005; Ye et al. 2009). During waking and REM sleep, it is known that the "specific" thalamocortical nuclei are excited by cholinergic input from the PPN; however, recent reports demonstrate that the Pf is more likely to be inhibited by cholinergic agents (Beatty et al. 2009; Ye et al. 2009). Thus we hypothesize that cholinergic PPN neurons sending efferents to the "nonspecific" Pf may be part of a feedback inhibitory circuit, thus disinhibiting the Pf during waking and REM sleep; meanwhile, those sending efferents to specific thalamocortical neurons could be part of a feedback excitatory circuit involved in thalamocortical activation. To confirm this hypothesis, more confined retrobead injections in different locations within the thalamus are required. Our experiments were conducted on neonatal rats, which introduced difficulties in limiting the injection to a certain thalamic nucleus. To determine the origins of GABAergic, glycinergic, and glutamatergic inputs, in the future, it may be necessary to perform lesions of specific nuclei with efferent GABAergic or glutamatergic projections to the PPN. Then the impact of such lesions on cholinergic modulation of fast synaptic transmission could be further investigated using whole cell patch clamp recordings.

Functional implications

Although the present study was conducted on brain slices, it provides significant insight to the understanding of mechanisms underlying in vivo observations on the influence of GABAergic and glutamatergic modulation of PPN neurons on sleep-wake cycles. It has been reported that activation of $GABA_A$ receptors on PPN neurons increase REM sleep in rat and cat (Pal and Mallick 2004, 2009; Torterolo et al. 2002). Meanwhile, microinjection of glutamate into the PPN increased the duration of waking and REM sleep (Datta et al. 2001b), and the increase in waking appeared to be due to the activation of NMDA receptors (Datta et al. 2001a), whereas, kainate receptors were involved in the induction of REM sleep (Datta 2002; Datta et al. 2002). Our finding that a cholinergic agonist could increase both GABA and glutamate release to PPN thalamic projecting neurons provides a neural substrate for these in vivo studies.

At the single cell level, the firing patterns and the membrane potential oscillations of PPN neurons, especially of those sending efferent projections to the thalamus, have considerable impact on the modulation of cortical arousal states. The present study showed that the cholinergic input could affect membrane responses in PPN output neurons not only by directly acting on postsynaptic receptors but also by acting indirectly via GABAergic, glycinergic, glutamatergic, and electrical synapses (Garcia-Rill et al. 2007). Interestingly, the frequencies of sIPSCs (~5 Hz) and sEPSCs (~7.7 Hz) in the presence of CAR, occur in the theta frequency range. Our previous study showed that the frequency of spikelets, which are indicative of electrical coupling and reflect the firing frequency of the coupled neuron, also falls in the theta range (Garcia-Rill et al. 2007). These findings are similar to CAR-induced theta oscillations in the hippocampus, which show concentration and temperature dependent properties (Dickinson et al. 2003; Fellous and Sejnowski 2000) and are modulated by electrical coupling (Konopacki et al. 2004), inhibitory interneurons (Chapman and Lacaille 1999; Reich et al. 2005), and glutamatergic inputs (D'Antuono et al. 2001). PPN neurons, however, may fire at higher frequencies, especially at gamma band frequency, when maximally activated or under the influence of combined cholinergic and glutamatergic inputs (C. Simon, N. Kezunovic, M. Ye, J. Hyde, A. Hayar, D. K. Williams, E. Garcia-Rill, unpublished data).

Theta and gamma oscillations have been recorded using EEG, intracellular, and extracellular recordings mainly in the hippocampus and neocortex. They are thought to represent an "on-line" state, are consistently present during REM sleep, and have been attributed to certain waking behaviors including navigation, exploration, and sensory perception as well as memory encoding and retrieval (Buzsaki 2005; Diekelmann and Born 2010; Lisman and Buzsaki 2008; Montgomery et al. 2008). Recently, it was reported that hippocampal theta oscillations could propagate as waves (Lubenov and Siapas 2009), indicating that the brain may use both spatial and temporal coding to accurately transmit and process such information. Also the amplitude of gamma oscillations induced by paired sensory stimuli appeared to be higher than when using single stimuli (Gross et al. 2007). This may shed some light on the induction of theta and gamma frequencies by sensory input to PPN.

Our study provides the first evidence for the presence of theta oscillations in the PPN, which can be independently modulated by electrical coupling, GABAergic and glutamatergic inputs. We propose that intrinsic membrane properties control the frequency of oscillations, which may be further modulated by fast chemical synapses; however, electrical synapses may be responsible for their coherence, which in turn promotes the propagation of synchronized rhythmic activity to the thalamus, and subsequently activates waking and REM sleep states (Garcia-Rill et al. 2007).

Downloaded from jn.physiology.org on August 15, 2010

Limitations

There are some limitations in this study that need to be recognized. First, our study was conducted on brain slices, which do not exhibit sleep-wake cycle, or perform other physiological functions, like movement. Therefore we cannot link single cell activity to their related functions in vivo. Our conclusions regarding physiological significance need to be considered with caution until confirmed in such preparations. Another limitation is that superfusion of brain slices with neuroactive agents activates all receptors on the slice so that we cannot distinguish whether different populations of neurons are active during different functional states or through different pathways. In addition, in vivo, there is more subtle control of inputs to a population of cells such that pre- versus postsynaptic effects may occur at different times rather than being concurrently activated as they are during superfusion. The third one is the difficulty in triple labeling cholinergic, glutamatergic, and GABAergic cells to determine the transmitter phenotype in every cell recorded. Unfortunately, only triple in situ hybridization, such as that reported recently identifying three separate (nonoverlapping) populations of PPN neurons (Wang and Morales 2009), may be necessary. In addition, the use of retrobeads for labeling output neurons allows us to determine if some of these cells are cholinergic (using bNOS immunocytochemistry as herein reported), but we are unable to distinguish between glutamatergic and possible GABAergic output neurons in the PPN. Making this distinction is important and may help us understand why cholinergic agents also produce mixed effects in the Pf (Beatty et al. 2009; Ye et al. 2009).

In summary, our study indicates that both inhibitory and excitatory fast synaptic transmission to PPN thalamic projecting neurons may be enhanced by cholinergic inputs. These findings advance our understanding of the intrinsic mechanisms underlying the regulation of thalamocortical arousal states by the brain stem reticular formation.

GRANTS

This work was supported by National Institutes of Health Grant R01 NS-020246-22 and by core facilities of the Center for Translational Neuroscience supported by NIH Grant P20 RR-020146-06.

REFERENCES

Beatty JA, Sylwestrak EL, Cox CL. Two distinct populations of projection neurons in the rat lateral parafascicular thalamic nucleus and their cholinergic responsiveness. *Neuroscience* 162: 155–173, 2009.

Buzsaki G. Theta rhythm of navigation: link between path integration and landmark navigation, episodic and semantic memory. *Hippocampus* 15: 827–840, 2005.

Chapman CA, Lacaille JC. Cholinergic induction of theta-frequency oscillations in hippocampal inhibitory interneurons and pacing of pyramidal cell firing. *J Neurosci* 19: 8637–8645, 1999.

Clements JR, Grant S. Glutamate-like immunoreactivity in neurons of the laterodorsal tegmental and pedunculopontine nuclei in the rat. *Neurosci Lett* 120: 70–73, 1990.

Curro Dossi R, Pare D, Steriade M. Short-lasting nicotinic and long-lasting muscarinic depolarizing responses of thalamocortical neurons to stimulation of mesopontine cholinergic nuclei. *J Neurophysiol* 65: 393–406, 1991.

D'Antuono M, Kawasaki H, Palmieri C, Avoli M. Network and intrinsic contributions to carbachol-induced oscillations in the rat subiculum. *J Neurophysiol* 86: 1164–1178, 2001.

Datta S. Evidence that REM sleep is controlled by the activation of brain stem pedunculopontine tegmental kainate receptor. *J Neurophysiol* 87: 1790–1798, 2002.

Datta S, Patterson EH, Spoley EE. Excitation of the pedunculopontine tegmental NMDA receptors induces wakefulness and cortical activation in the rat. *J Neurosci Res* 66: 109–116, 2001a.

Datta S, Siwek DF. Single cell activity patterns of pedunculopontine tegmentum neurons across the sleep-wake cycle in the freely moving rats. *J Neurosci Res* 70: 611–621, 2002.

Datta S, Siwek DF, Patterson EH, Cipolloni PB. Localization of pontine PGO wave generation sites and their anatomical projections in the rat. *Synapse* 30: 409–423, 1998.

Datta S, Spoley EE, Mavanji VK, Patterson EH. A novel role of pedunculopontine tegmental kainate receptors: a mechanism of rapid eye movement sleep generation in the rat. *Neuroscience* 114: 157–164, 2002.

Datta S, Spoley EE, Patterson EH. Microinjection of glutamate into the pedunculopontine tegmentum induces REM sleep and wakefulness in the rat. *Am J Physiol Regulatory Integrative Comp Physiol* 280: R752–759, 2001b.

Deurveilher S, Hennevin E. Lesions of the pedunculopontine tegmental nucleus reduce paradoxical sleep (PS) propensity: evidence from a short-term PS deprivation study in rats. *Eur J Neurosci* 13: 1963–1976, 2001.

Dickinson R, Awaiz S, Whittington MA, Lieb WR, Franks NP. The effects of general anaesthetics on carbachol-evoked gamma oscillations in the rat hippocampus in vitro. *Neuropharmacology* 44: 864–872, 2003.

Diekelmann S, Born J. The memory function of sleep. *Nat Rev Neurosci* 11: 114–126, 2010.

Dun NJ, Dun SL, Forstermann U. Nitric oxide synthase immunoreactivity in rat pontine medullary neurons. *Neuroscience* 59: 429–445, 1994.

Erro E, Lanciego JL, Gimenez-Amaya JM. Relationships between thalamostriatal neurons and pedunculopontine projections to the thalamus: a neuroanatomical tract-tracing study in the rat. *Exp Brain Res* 127: 162–170, 1999.

Fellous JM, Sejnowski TJ. Cholinergic induction of oscillations in the hippocampal slice in the slow (0.5–2 Hz), theta (5–12 Hz), and gamma (35–70 Hz) bands. *Hippocampus* 10: 187–197, 2000.

Ford B, Holmes CJ, Mainville L, Jones BE. GABAergic neurons in the rat pontomesencephalic tegmentum: codistribution with cholinergic and other tegmental neurons projecting to the posterior lateral hypothalamus. *J Comp Neurol* 363: 177–196, 1995.

Fort P, Luppi PH, Jouvet M. Glycine-immunoreactive neurons in the cat brain stem reticular formation. *Neuroreport* 4: 1123–1126, 1993.

Garcia-Rill E, Heister DS, Ye M, Charlesworth A, Hayar A. Electrical coupling: novel mechanism for sleep-wake control. *Sleep* 30: 1405–1414, 2007.

Good CH, Bay KD, Buchanan R, Skinner RD, Garcia-Rill E. Muscarinic and nicotinic responses in the developing pedunculopontine nucleus (PPN). *Brain Res* 1129: 147–155, 2007.

Granata AR, Kitai ST. Inhibitory substantia nigra inputs to the pedunculopontine neurons. *Exp Brain res Exp Hirnforsch* 86: 459–466, 1991.

Gross J, Schnitzler A, Timmermann L, Ploner M. Gamma oscillations in human primary somatosensory cortex reflect pain perception. *PLoS Biol* 5: e133, 2007.

Heister DS, Hayar A, Garcia-Rill E. Cholinergic modulation of GABAergic and glutamatergic transmission in the dorsal subcoeruleus: mechanisms for REM sleep control. *Sleep* 32: 1135–1147, 2009.

Hobson JA, Pace-Schott EF. The cognitive neuroscience of sleep: neuronal systems, consciousness and learning. *Nat Rev Neurosci* 3: 679–693, 2002.

Kamondi A, Williams JA, Hutcheon B, Reiner PB. Membrane properties of mesopontine cholinergic neurons studied with the whole-cell patch-clamp technique: implications for behavioral state control. *J Neurophysiol* 68: 1359–1372, 1992.

Kang Y, Kitai ST. Electrophysiological properties of pedunculopontine neurons and their postsynaptic responses following stimulation of substantia nigra reticulata. *Brain Res* 535: 79–95, 1990.

Kha HT, Finkelstein DI, Pow DV, Lawrence AJ, Horne MK. Study of projections from the entopeduncular nucleus to the thalamus of the rat. *J Comp Neurol* 426: 366–377, 2000.

Kim J, Nakajima K, Oomura Y, Wayner MJ, Sasaki K. Electrophysiological effects of orexins/hypocretins on pedunculopontine tegmental neurons in rats: an in vitro study. *Peptides* 30: 191–209, 2009.

Kobayashi T, Good C, Biedermann J, Barnes C, Skinner RD, Garcia-Rill E. Developmental changes in pedunculopontine nucleus (PPN) neurons. *J Neurophysiol* 91: 1470–1481, 2004.

Kobayashi T, Homma Y, Good C, Skinner RD, Garcia-Rill E. Developmental changes in the effects of serotonin on neurons in the region of the pedunculopontine nucleus. *Brain Res Dev Brain Res* 140: 57–66, 2003.

Downloaded from jn.physiology.org on August 15, 2010

Kobayashi S, Nakamura Y. Synaptic organization of the rat parafascicular nucleus, with special reference to its afferents from the superior colliculus and the pedunculopontine tegmental nucleus. *Brain Res* 980: 80–91, 2003.

Kohlmeier KA, Wess J, Bickford ME, Leonard CS. Multiple inhibitory actions mediated by muscarinic M2 and M4 receptors in mesopontine cholinergic neurons. *Soc Neurosci Abstr* 33: 735.7, 2007.

Konopacki J, Kowalczyk T, Golebiewski H. Electrical coupling underlies theta oscillations recorded in hippocampal formation slices. *Brain Res* 1019: 270–274, 2004.

Lacey CJ, Bolam JP, Magill PJ. Novel and distinct operational principles of intralaminar thalamic neurons and their striatal projections. *J Neurosci* 27: 4374–4384, 2007.

Leonard CS, Llinas R. Electrophysiology of mammalian pedunculopontine and laterodorsal tegmental neurons in vitro: implications for the control of REM sleep. In: *Brain Cholinergic Systems*, edited by Steriade M and Biesold D. Oxford, UK: Oxford Science, 1990.

Leonard CS, Llinas R. Serotonergic and cholinergic inhibition of mesopontine cholinergic neurons controlling REM sleep: an in vitro electrophysiological study. *Neuroscience* 59: 309–330, 1994.

Lisman J, Buzsaki G. A neural coding scheme formed by the combined function of gamma and theta oscillations. *Schizophr Bull* 34: 974–980, 2008.

Llinas R, Ribary U. Consciousness and the brain. The thalamocortical dialogue in health and disease. *Ann NY Acad Sci* 929: 166–175, 2001.

Lubenov EV, Siapas AG. Hippocampal theta oscillations are traveling waves. *Nature* 459: 534–539, 2009.

McCormick DA. Cellular mechanisms underlying cholinergic and noradrenergic modulation of neuronal firing mode in the cat and guinea pig dorsal lateral geniculate nucleus. *J Neurosci* 12: 278–289, 1992.

McCormick DA, Prince DA. Actions of acetylcholine in the guinea-pig and cat medial and lateral geniculate nuclei, in vitro. *J Physiol* 392: 147–165, 1987.

Mena-Segovia J, Sims HM, Magill PJ, Bolam JP. Cholinergic brain stem neurons modulate cortical gamma activity during slow oscillations. *J Physiol* 586: 2947–2960, 2008.

Mineff EM, Popratiloff A, Romansky R, Kazakos V, Kaimaktschieff V, Usunoff KG, Ovtscharoff W, Marani E. Evidence for a possible glycinergic inhibitory neurotransmission in the midbrain and rostral pons of the rat studied by gephyrin. *Arch Physiol Biochem* 106: 210–220, 1998.

Montgomery SM, Sirota A, Buzsaki G. Theta and gamma coordination of hippocampal networks during waking and rapid eye movement sleep. *J Neurosci* 28: 6731–6741, 2008.

Moruzzi G, Magoun HW. Brain stem reticular formation and activation of the EEG. *Electroencephalogr Clin Neurophysiol* 1: 455–473, 1949.

Pal D, Mallick BN. GABA in pedunculo pontine tegmentum regulates spontaneous rapid eye movement sleep by acting on GABAA receptors in freely moving rats. *Neurosci Lett* 365: 200–204, 2004.

Pal D, Mallick BN. GABA in pedunculopontine tegmentum increases rapid eye movement sleep in freely moving rats: possible role of GABA-ergic inputs from substantia nigra pars reticulata. *Neuroscience* 164: 404–414, 2009.

Parent M, Descarries L. Acetylcholine innervation of the adult rat thalamus: distribution and ultrastructural features in dorsolateral geniculate, parafascicular, and reticular thalamic nuclei. *J Comp Neurol* 511: 678–691, 2008.

Phelan KD, Mahler HR, Deere T, Cross CB, Good C, Garcia-Rill E. Postnatal maturational properties of rat parafascicular thalamic neurons recorded in vitro. *Thalamus Related Syst* 3: 89–113, 2005.

Reich CG, Karson MA, Karnup SV, Jones LM, Alger BE. Regulation of IPSP theta rhythm by muscarinic receptors and endocannabinoids in hippocampus. *J Neurophysiol* 94: 4290–4299, 2005.

Saitoh K, Hattori S, Song WJ, Isa T, Takakusaki K. Nigral GABAergic inhibition upon cholinergic neurons in the rat pedunculopontine tegmental nucleus. *Eur J Neurosci* 18: 879–886, 2003.

Sakai K, el Mansari M, Jouvet M. Inhibition by carbachol microinjections of presumptive cholinergic PGO-on neurons in freely moving cats. *Brain Res* 527: 213–223, 1990.

Semba K, Fibiger HC. Afferent connections of the laterodorsal and the pedunculopontine tegmental nuclei in the rat: a retro- and antero-grade transport and immunohistochemical study. *J Comp Neurol* 323: 387–410, 1992.

Steininger TL, Rye DB, Wainer BH. Afferent projections to the cholinergic pedunculopontine tegmental nucleus and adjacent midbrain extrapyramidal area in the albino rat. I. Retrograde tracing studies. *J Comp Neurol* 321: 515–543, 1992.

Steriade M, Pare D, Datta S, Oakson G, Curro Dossi R. Different cellular types in mesopontine cholinergic nuclei related to ponto-geniculo-occipital waves. *J Neurosci* 10: 2560–2579, 1990.

Stevens DR, McCarley RW, Greene RW. Excitatory amino acid-mediated responses and synaptic potentials in medial pontine reticular formation neurons of the rat in vitro. *J Neurosci* 12: 4188–4194, 1992.

Sugaya K, McKinney M. Nitric oxide synthase gene expression in cholinergic neurons in the rat brain examined by combined immunocytochemistry and in situ hybridization histochemistry. *Brain Res Mol Brain Res* 23: 111–125, 1994.

Takakusaki K, Shiroyama T, Kitai ST. Two types of cholinergic neurons in the rat tegmental pedunculopontine nucleus: electrophysiological and morphological characterization. *Neuroscience* 79: 1089–1109, 1997.

Takakusaki K, Shiroyama T, Yamamoto T, Kitai ST. Cholinergic and noncholinergic tegmental pedunculopontine projection neurons in rats revealed by intracellular labeling. *J Comp Neurol* 371: 345–361, 1996.

Torterolo P, Morales FR, Chase MH. GABAergic mechanisms in the pedunculopontine tegmental nucleus of the cat promote active (REM) sleep. *Brain Res* 944: 1–9, 2002.

Vilaro MT, Palacios JM, Mengod G. Multiplicity of muscarinic autoreceptor subtypes? Comparison of the distribution of cholinergic cells and cells containing mRNA for five subtypes of muscarinic receptors in the rat brain. *Brain Res Mol Brain Res* 21: 30–46, 1994.

Vilaro MT, Wiederhold KH, Palacios JM, Mengod G. Muscarinic M2 receptor mRNA expression and receptor binding in cholinergic and noncholinergic cells in the rat brain: a correlative study using in situ hybridization histochemistry and receptor autoradiography. *Neuroscience* 47: 367–393, 1992.

Wang HL, Morales M. Pedunculopontine and laterodorsal tegmental nuclei contain distinct populations of cholinergic, glutamatergic and GABAergic neurons in the rat. *Eur J Neurosci* 29: 340–358, 2009.

Ye M, Hayar A, Garcia-Rill E. Cholinergic responses and intrinsic membrane properties of developing thalamic parafascicular neurons. *J Neurophysiol* 102: 774–785, 2009.

Zhu JJ, Uhlrich DJ. Cellular mechanisms underlying two muscarinic receptor-mediated depolarizing responses in relay cells of the rat lateral geniculate nucleus. *Neuroscience* 87: 767–781, 1998.

Downloaded from jn.physiology.org on August 15, 2010